



University of Tennessee, Knoxville
Trace: Tennessee Research and Creative Exchange

Masters Theses

Graduate School

8-2008

Relationship between Slug-Test and Effective Hydraulic Conductivities for 2-Dimensional Heterogeneous Aquifers

Richard Walker Donat
University of Tennessee - Knoxville

Recommended Citation

Donat, Richard Walker, "Relationship between Slug-Test and Effective Hydraulic Conductivities for 2-Dimensional Heterogeneous Aquifers." Master's Thesis, University of Tennessee, 2008.
https://trace.tennessee.edu/utk_gradthes/3644

This Thesis is brought to you for free and open access by the Graduate School at Trace: Tennessee Research and Creative Exchange. It has been accepted for inclusion in Masters Theses by an authorized administrator of Trace: Tennessee Research and Creative Exchange. For more information, please contact trace@utk.edu.

To the Graduate Council:

I am submitting herewith a thesis written by Richard Walker Donat entitled "Relationship between Slug-Test and Effective Hydraulic Conductivities for 2-Dimensional Heterogeneous Aquifers." I have examined the final electronic copy of this thesis for form and content and recommend that it be accepted in partial fulfillment of the requirements for the degree of Master of Science, with a major in Geology.

Edmund Perfect, Major Professor

We have read this thesis and recommend its acceptance:

Randall W. Gentry, Larry D. McKay

Accepted for the Council:

Dixie L. Thompson

Vice Provost and Dean of the Graduate School

(Original signatures are on file with official student records.)

To the Graduate Council:

I am submitting herewith a thesis written by Richard Walker Donat entitled "Relationship between Slug-Test and Effective Hydraulic Conductivities for 2-Dimensional Heterogeneous Aquifers." I have examined the final electronic copy of this thesis for form and content and recommend that it be accepted in partial fulfillment of the requirements for the degree of Master of Science, with a major in Geology.

Edmund Perfect, Major Professor

We have read this thesis
and recommend its acceptance:

Randall W. Gentry

Larry D. McKay

Accepted for the Council:

Carolyn R. Hodges, Vice Provost and
Dean of the Graduate School

**Relationship between Slug-Test and Effective Hydraulic
Conductivities for 2-Dimensional Heterogeneous Aquifers**

A Thesis Presented for the
Master of Science Degree
The University of Tennessee, Knoxville

Richard Walker Donat
August 2008

Abstract

Slug tests are one of the most common field tests used by hydrogeologists to evaluate the hydraulic conductivity of an aquifer system. Steady-state and transient (slug test) numerical simulations were run in 37, 2-dimensional randomized multifractal hydraulic conductivity fields. Each field consisted of 59,049 individual saturated hydraulic conductivity (K) values with varying numbers of hydrofacies and different degrees of spatial heterogeneity. The K_{eff} values were determined by examining the flux in and out of the steady-state numerical model. The K_{slug} values were determined by adding a slug of water to the center node of the field and evaluating the numerical head response over time with the Cooper-Bredehoeft-Papadopoulos method. The zone of influence of the slug test was also measured for each realization. The variance of $\ln(K_{\text{slug}})$ decreased as the zone of influence increased. K_{eff} and K_{slug} were determined on 100 realizations of a specific multifractal field. The K_{slug} values followed a distribution similar to that of the field hydraulic conductivity values, while the K_{eff} values exhibited a much narrower distribution. Linear regression analyses of $\ln(K_{\text{eff}})$ on $\ln(K_{\text{slug}})$ were performed to evaluate how well the slug test values predicted the effective saturated hydraulic conductivity at each individual scale and over all scales. The results of these regression analyses showed that $\ln(K_{\text{slug}})$ underestimates the hydraulic conductivity in low hydraulic conductivity material with high K inclusions and overestimates the hydraulic conductivity in extremely high hydraulic conductivity fields with low K inclusions. Averaging three replicate measurements of $\ln(K_{\text{slug}})$ resulted in a significant reduction of error associated with the prediction of $\ln(K_{\text{eff}})$. The mean absolute difference between $\ln(K_{\text{eff}})$ and $\ln(K_{\text{slug}})$ also decreased as the size of the hydrofacies decreased.

Table of Contents

Section	page
1.0 Introduction	1
1.1 Literature Review	2
1.2 Goal	7
1.3 Objectives	7
2.0 Methodology	8
2.1 Generating Random Multifractal Fields	9
2.2 Modeling Software	10
2.2.1 Steady-State Numerical Simulations	10
2.2.2 Transient Numerical Slug Test Simulations	11
2.2.3 Cooper-Bredehoeft-Papadopulos Analytical Solution	12
2.3 Zone of Influence	14
2.4 Anisotropy	14
2.5 Statistical Methods	15
2.6 Multiple Random Realizations	16
3.0 Results and Discussion	17
3.1 Detailed Examination of a Specific Multifractal Field	18
3.2 Steady-State Results	18
3.3 Slug Test Results	20
3.4 Steady-State and Slug Test Results Compared	22
3.4.1 Correlations	22
3.4.2 Regression Analyses Over All Replications, p and i Level	22
3.4.3 Regression Analyses Based on the Averages of Replications Over p and i Levels	23
3.4.4 Regression Analyses at Each i Level	24
4.0 Conclusions and Further Research	26
Works Cited	30-35
Appendices A-E	36-66
Vita	67

List of Tables

No.		page
A.1	Residual sums of squares for nonlinear fits of head response data in AQTESOLV	37
A.2	Mean, variance, and normality test for the $p=4/9$, $i=5$, $b=3$ multifractal field	38
A.3	ANOVA table significance levels for $\ln(K_{\text{eff}})$, λ_{eff} , $\ln(K_{\text{slug}})$, λ_r , and r_{norm}	38
A.4	Variance of $\ln(K_{\text{eff}})$	38
A.5	Variance of $\ln(K_{\text{slug}})$	39
A.6	Regression models ($y=mx+b$) for the $\ln(\text{mean})$ and $\ln(\text{variance})$ of $\ln(K_{\text{slug}})$ versus $\ln(r_{\text{norm}})$	39
A.7	Correlation Matrix of $\ln(K_{\text{eff}})$, λ_{eff} , $\ln(K_{\text{slug}})$, r_{norm} , and λ_r	39
A.8	Linear regression model ($y=mx+b$) showing the slope, intercept, R^2 , MAPE, and number of observations for each i level for all of the realizations	40
A.9	Linear regression model ($y=mx+b$) showing the slope, intercept, R^2 , MAPE, and number of observations for each i level based on averages of the realizations	40

List of Tables (Continued)

No.		page
A.10	In transformed median values for the multifractal fields	40

List of Figures

No.		page
B.1	Deterministic 2-dimensional multifractal field for $p=8/9$, $i=5$, $b=3$ (left) and random 2-dimensional multifractal field for $p=8/9$, $i=5$, $b=3$ (right)	41
B.2	Six different scales for a $p=8/9$, $b=3$ random 2-d multifractal field. From top left to bottom right: $i=1$, $i=2$, $i=3$, $i=4$, $i=5$, $i=6$. Black cells: low K , white cells: high K	41
B.3	Boundary conditions for the steady-state flow simulations. Steady-state flow in the x direction (left) and steady-state flow in the y direction (right)	42
B.4	Example head distributions with contour intervals of 0.1 for steady-state flow in the x direction for random 2-d multifractal fields: $p=8/9$, $i=5$, $b=3$ (left) and $p=5/9$, $i=5$, $b=3$ (right)	42
B.5	Example AQTESOLV non-linear regression fit for head response data	43
B.6	Relationship between $\ln(K_{\text{eff}})$ and $\ln(K_{\text{slug}})$ with r_c optimized for 40 homogeneous fields	43
B.7	Measurement of the zone of influence in the x and y directions for the transient slug test simulations	44
B.8	Histograms of 100 realizations of K_{eff} and K_{slug} and 59,049 K field values for the $p=4/9$, $i=5$, $b=3$ multifractal field	44

List of Figures (Continued)

No.		page
B.9	Mean values for K_{eff} with associated Tukey values by i level. Means with the same letter, within an i-level, are not significantly different at $p < 0.05$	45
B.10	Mean values for K_{slug} with associated Tukey values by i level Means with the same letter, within an i-level, are not significantly different at $p < 0.05$	46
B.11	Mean values for r_{norm} associated with the transient simulations and with associated Tukey values by i level. Means with the same letter, within an i-level, are not significantly different at $p < 0.05$	47
B.12	Plot of the average values of $\ln(K_{\text{slug}})$ versus $\ln(r_{\text{norm}})$ over all p and i levels	48
B.13	Plot of the ln transformed variance of $\ln(K_{\text{slug}})$ versus $\ln(r_{\text{norm}})$	49
B.14	Linear regression plots for all realizations with the 1 to 1 line (Top). Magnification of the linear regression plot from (-5,-5) (Bottom)	50
B.15	Linear regression plots for an average of the realizations with the 1 to 1 line (Top). Magnification of the linear regression plot from (-5,-5) (Bottom)	51

List of Figures (Continued)

No.		page
B.16	Linear regression plots for an average of the realizations of the $\ln(K_{\text{eff}})$ values with the corresponding $\ln(\text{Median})$ values with the 1 to 1 line (Top). Magnification of the linear regression plot from (-5,-5) (Bottom)	52

1.0 Introduction

1.1 Literature Review

Hydraulic conductivity (K) is an important hydrogeologic parameter used in predicting flow and solute transport in soils, sediments, and rocks. It can be used to estimate and determine such things as spreading velocities of contaminant plumes, aquifer yield and sustainability, and effectiveness of aquitards as barriers to movement of contaminants. Techniques that are often used in estimating hydraulic conductivity include grain size analysis, permeameter tests using core samples, pumping tests, and slug tests. Measurements used to determine the hydraulic conductivity of a material differ by the measurement technique and the scale of measurement. Furthermore, there are numerous analytical solutions that can be used to determine K based on pumping and slug test response data. Each of these analytical solutions can yield different estimations of K , even for the same data set. Therefore it is important to develop a better understanding of the effectiveness of well response tests and their associated analytical solutions.

One of the most common field tests used to quantify small scale hydrogeologic characteristics of aquifers is the slug test. This is mainly because of its ease of implementation and affordability of the test. Many advances have been made to correct for the errors incorporated into hydraulic parameters determined using slug tests (Butler, 1996). One of the most effective tests to measure large scale hydraulic conductivity in the field is the pumping test. Thus, a logical question to ask is: how does K_{pump} (pumping test hydraulic conductivity) compare to K_{slug} (slug test hydraulic conductivity).

Butler and Healey (1998) show, that in most cases, the value for K_{pump} is greater than K_{slug} due to well skin effects, incomplete well development, and vertical anisotropy. Rovey and Cherkauer (1995) proposed that the underestimation of K_{pump} by K_{slug} is largely due to scaling effects. They suggest that that small scale

slug tests are not able to adequately measure the influence of high hydraulic conductivity pockets in the aquifer. Rovey (1998) examined scaling effects associated with slug, pumping, and pressure injection tests in a numerical model. Rovey and Niemann (2001) and Shulze-Makuch et al. (1999) showed how measured values of hydraulic conductivity increase with scale for different types of porous media.

Another important issue is the variability of different measurements of K_{slug} and K_{pump} . Vargas and Ortega-Guerrero (2004) and Loáiciga et al. (2006) observed substantial spatial variability in K_{slug} , even in apparently homogeneous formations. Lee and Lee (1999) showed that K_{slug} has a greater variability than K_{pump} . In contrast, Chapius et al. (2005) demonstrated that, in a quasi-homogeneous aquifer, distributions of K_{slug} and K_{pump} are narrow in range and similar. Therefore it is becoming increasingly important to study K_{slug} and understand how well it represents the larger scale hydraulic conductivity values for various aquifer systems.

The effects of heterogeneity, due to spatial variations in hydrofacies, have been studied exhaustively. Sanchez-Vila et al. (2006) reviewed work from the past 30 years addressing the issue of heterogeneity. One of the most important facets brought up in that review is determining representative values of hydraulic conductivity. It is very difficult in a field environment to ever know the true value of the hydraulic conductivity. Hence it is important to study how accurately different hydraulic conductivity estimation methods are able to estimate the effective hydraulic conductivity (K_{eff}) of aquifers with varying levels of heterogeneity. The K_{eff} is the expected value of the flux and head gradient, which can give a regional value of hydraulic conductivity for an aquifer system (Sanchez-Vila et al., 2006). Since the effective hydraulic conductivity cannot be measured with 100% accuracy in the field it is useful to employ groundwater

models to estimate this value and compare it to values of K obtained from head response tests (i.e. K_{pump} and/or K_{slug}).

Ground water models have increased in popularity with the availability of innovative new software and the increase in computing power (Bredehoeft, 2006). Modeling software allows users to input a wide variety of hydrogeologic parameters, such as recharge, hydraulic conductivity, rivers, evapotranspiration, storage, vertical leakage, aquifer types (confined or unconfined), geologic boundaries, effective porosity, and specific yield to simulate natural groundwater systems. From this information the user can evaluate steady-state and/or transient simulations to examine chemical migration, effective hydraulic conductivity, missing hydrogeologic parameters, aquifer yield, influence of pumping on wetlands, and a variety of other phenomena. Numerical simulations in groundwater modeling allow the modeler to analyze specific tests without exposure to some of the problems that one encounters in field environments (Butler et al., 1996). When modeling is used properly it can give a wealth of information that would often be difficult to determine under field conditions.

There are many different types of approaches to model aquifer heterogeneity; these include, but are not limited to, geostatistical methods, the Boolean method, and genetic methods (for more information on these methods the reader is referred to Marsily et al., 1998). Eaton (2006) also described methods (continuum and discrete paradigms, zonal and geostatistical approaches) for modeling heterogeneity and their respective advantages. Another approach that is often seen in the literature is the use of assigning hydraulic conductivity values to model cells in order to represent fracture patterns or block heterogeneity; such patterns are usually assumed to be Euclidean (Osiensky et al., 2000; Rovey, 1998). For example, Osiensky et al. (2000) used 16 large blocks of transmissivity values and simulated pumping tests in order to evaluate how the transmissivity

values changed with respect to whether the late or early drawdown data were examined.

As defined in Turcotte (1997), fractals are patterns that repeat themselves and are quantified by a fractional dimension while multifractals are a sequence of fractal dimensions derived from the moments of a statistical distribution. According to recent analyses of field data, it has been suggested that saturated hydraulic conductivity distributions of rocks and soils are multifractal in nature (Neuman and Diferico et al., 2003, and Molz et al., 2004). Multifractal scaling of the spatial distribution of hydraulic conductivity has been validated with analyses presented in Liu and Molz (1997), Boufadel et al. (2000), and Tennekoon et al. (2003). For example, Tennekoon et al. (2003) studied several field sites in order to examine the scaling properties of K . They found that their multifractal model was able to produce the probability distribution of K seen at those field sites. For these reasons investigating the scaling of known multifractal models can result in an improved understanding of the influence of heterogeneity on K_{eff} in aquifers.

Various types of numerical flow simulations have been performed in fractal and multifractal fields. Some of these include, Hassan et al. (1997) who ran flow and transport simulations in order to study migration of chemicals at different levels of heterogeneity in fractal fields. Babadagli (2006) measured and compared the effective permeability of 2-d fractal fields using numerical simulations and averaging techniques. Lenormand et al. (1990) developed anisotropic multifractal fields to compare two-phase flow patterns from model simulations with data from real flow experiments. Veneziano and Essiam (2003) ran flow simulations in stochastic multifractal log normal fields to study the effect of variability in K on the hydraulic gradient and the specific flow. Dreuzy et al.

(2004) studied diffusion in heterogeneous randomly continuous multifractal media.

Koirala et al. (2008) studied the scaling of K_{eff} for random multifractal K fields based on the earlier work of Perfect et al. (2006). Their approach involved generating multifractal 2-dimensional Sierpinski Carpets consisting of normalized mass fractions calculated from the truncated Binomial distribution. These researchers focused on two main goals: exploring how the frequency distribution of hydraulic conductivity changes as a function of the probability of carpet formation (p) and scale (i), and how the effective hydraulic conductivity varies at different scales for dissimilar probabilities of carpet formation. The p value is a statistical property that determines the level of heterogeneity for a 2-d multifractal field while the i value reflects the resolution of the multifractal field. As the i value is decreased the multifractal field decreases in resolution and number of hydrofacies. In Koirala et al. (2008) the average effective hydraulic conductivity of three realizations of each multifractal field was determined for probabilities ranging from 1/9 to 8/9 based on numerical steady-state simulations. These researchers determined that, as the probability value increases so does the effective hydraulic conductivity, and that lower p -values best represent the scaling behavior of more heterogeneous hydraulic conductivity fields. Koirala et al. (2008) also suggested a relationship between the different multifractal hydraulic conductivity fields and natural hydrogeological systems.

The multifractal approach appears to have some advantages for modeling hydraulic conductivity fields. It enables a model to capture an accurate and detailed representation of the heterogeneity commonly seen in field environments, and can be directly applied and compared to natural systems. Although many flow simulations have been run for different types of fractal and

multifractal fields none, to this author's knowledge, have compared numerous steady-state simulations with head response simulations, specifically the slug test.

1.2 Goal

The main focus of this thesis is to examine the ability of small scale head response tests (slug tests) to estimate larger scale effective hydraulic conductivity values in multifractal fields that range in levels of heterogeneity, contain low and high hydraulic conductivity values, and whose hydrofacies have different length scales.

1.3 Objectives

The main objectives of this project are to: (1) compare all values and the averages of three replications of K_{eff} with K_{slug} over a range of 2-dimensional multifractal fields and scales, (2) determine regression equations for all realizations and the averages of the replications as a function of i level to better understand how accurately small scale slug tests predict K_{eff} , and (3) examine a specific 2-d multifractal field ($p=4/9$, $b=3$, $i=5$) in detail to determine relationships between the distributions of K_{eff} and K_{slug} , and the probability distribution of the K values in the field (K_{field}).

2.0 Methodology

2.1 Generating Random Multifractal Fields

The method undertaken to generate and upscale effective saturated hydraulic conductivities is taken from Perfect et al. (2006) and Koirala et al. (2008). This method involves normalizing mass fractions calculated from a truncated binomial distribution for a wide variety of probability distribution values (p) with a scale factor (b), and different iteration (i) levels.

The MATLAB code used to construct the 2-d multifractal fields was a modified version of the code developed by Jung Woo-Kim (Koirala et al., 2008) (Appendix C). The MATLAB code allows one to input a scaling factor (b), a probability value (p), an iteration level (i), and choose the output to be a deterministic or a random multifractal field (Figure B.1). An $i=5$ multifractal field is a 243 by 243 matrix of 59,049 K values: whereas, an $i=1$ multifractal field is a 3 by 3 matrix with only 9 K values (Figure B.2). The modification of the MATLAB code takes the $i=1$, 3 by 3, matrix and divides each of the cells into 81 parts for the specific 9 K values represented; hence expanding the original matrix into a 243 by 243 matrix, while maintaining the respective characteristics of the original 3 by 3 matrix. This process was performed so that each of the multifractal fields contained the same number of cells for each i level enabling one to examine the large and small scale variations in hydraulic conductivity.

For this research p was varied between $1/9$ and $8/9$, $b=3$, and $i=1, 2...5$. Here $p=8/9$ represents a homogeneous high K field with a few low K inclusions and as one decreases the p -level to $p=1/9$ the fields become more heterogeneous with low K values and a few high K inclusions. The ranges of K values in the fields were from 0 to 1 and are represented as meters/second. To increase the resolution, in order to study scaling effects, the generator is simply applied to itself at different iterative values. The i level can be related to the spatial variation of K for geologic materials through the length scale of the hydrofacies,

i.e. $1/b^i$. For $b=3$, $i=5$ the K value changes at every grid cell, while at $i=4$ the change is at every 3 cells, $i=3$ at 9 cells, $i=2$ at 27 cells, and $i=1$ at 81 cells. Finally, each realization was randomized to represent different spatial heterogeneities.

2.2 Modeling Software

All slug test numerical simulations were run in Processing Modflow 5.30 (Chiang and Kinzelbach, 2001). The steady-state simulations were run in both Processing Modflow 5.30 (Chiang and Kinzelbach, 2001), and Argus One (MODFLOW GUI version 4) (Winston, 2000). Processing MODFLOW 5.30 had limited capabilities in solving for K_{eff} in the lower p -value multifractal fields. Therefore Argus One simulations were performed to determine the steady-state K_{eff} for the following multifractal fields: $p=2/9$, $i=5, 4$, and $p=1/9$, $i=5, 4, 3$. Steady-state flow simulations were run in both Argus One and Processing Modflow 5.30, for selected high p value fields, in order to compare the solved K_{eff} values for each software package. The K_{eff} values for the compared fields were the same, which validates the use of Argus One for solving for K_{eff} in the lower p -value fields. Both modeling software packages had difficulty in converging to a solution for the following fields: $p=1/9$, $i=5, 4, 3$. Therefore the results for these combinations were not used.

2.2.1 Steady-State Numerical Simulations

For the steady-state simulations the effective hydraulic conductivities in the x direction ($K_{x,eff}$) and y direction ($K_{y,eff}$) were evaluated in units of meters/second for three different random realizations for each of the 37 different multifractal fields. The boundary conditions for the model were no flow boundaries in either the x or y direction with a gradient in the y direction or x direction respectively (Figure B.3). The aquifers consisted of 59,049 discretized cells. Effective hydraulic conductivities were then solved by examining the fluxes in and fluxes out of the

steady-state simulations using a finite difference approach (Renard and de Marsily, 1997). Other than the $p=1/9$, $i=5$, 4 , 3 fields all of the simulations converged. The majority of the water budget errors for the simulations were 0% and none exceeded 3%. Once the models converged K_{eff} was calculated from the equilibrium fluxes based on Darcy's law (Fetter, 2001):

$$K_{eff} = -q \frac{\partial x}{\partial h} \dots\dots\dots(1)$$

where q is the flux, h is the hydraulic head and x is the length. Figure B.4 shows examples of the head changes for two multifractal fields. The mean effective hydraulic conductivity (K_{eff}) for a field was calculated as the geometric mean of $K_{y,eff}$ and $K_{x,eff}$.

2.2.2 Transient Numerical Slug Test Simulations

For the transient simulations the hydraulic conductivity was measured via the slug test method. The boundaries conditions for the matrix consisted of a constant head of 10 meters along the edge of the field. All cells received a value of 10 meters for the initial hydraulic head with the exception of the center node, which received a value of 11 meters to simulate a slug of water. The layer type was a confined aquifer with recharge only coming from the constant head boundaries. Specific storage and the storage coefficient for the model was $0.001m^{-1}$ in all grid cells except for the center node which was given a value of $1m^{-1}$ in order to simulate an open borehole. A Preconditioned Conjugate-Gradient 2 (PCG2) package was used in order to solve the Neuman series polynomials and a time step multiplier of 1.2 was employed so that more early time head response data in the well could be collected. Equation 2 is the governing equation for transient groundwater flow expressed in radial coordinates is (Fetter, 2001):

$$\frac{\partial^2 h}{\partial r^2} + \frac{1}{r} \frac{\partial h}{\partial r} = \frac{S}{T} \frac{\partial h}{\partial t} \dots\dots\dots(2)$$

where t is time, r is the radial distance, S is the storativity, and T is the transmissivity. After evaluating each simulation the water budget was checked for any discrepancies. A percent discrepancy of no more than 0.5%, was taken as an acceptable cut off limit by the author for the transient simulation (McDonald and Harbaugh, 1988). If the percent discrepancy was over 0.5% the water budget output file is documented in Appendix D. As the p-values decreased the solver had a more difficult time in producing a low percent discrepancy. It is important to note, however, that this did not appear to affect the estimated value of K_{slug} . This is probably due to the fact that the percent discrepancies are so small in value that they had no bearing on the head changes being recorded in the well used for the test. This concept was tested by allowing greater than 0.5% discrepancy and looking at a zero percent discrepancy for the same p-value, i-value, and realization. The results showed that there were no significant differences between the large percent discrepancy and the small percentage discrepancy for K_{slug} in the same multifractal field. The head change over time was identical for a larger percent error as it was for a zero percent error.

2.2.3 Cooper-Bredehoeft-Papadopulos Analytical Solution

The Cooper-Bredehoeft-Papadopulos method was the model chosen for analyzing the numerical slug test data under the following assumptions: that the aquifer is homogeneous, isotropic, confined, of uniform thickness, and screened the full length of the aquifer (Cooper et al., 1967). These assumptions are often ignored in the real world. This method involves matching the head divided by the initial head as a function of time to the type curves of Cooper et al. (1967). The equation used to solve for the transmissivity is as follows (Cooper et al., 1967):

$$T = \left(\frac{cr_c^2}{t_m} \right) \dots\dots\dots(3)$$

Here c_x represents the value obtained from overlying the type curve, r_c is the radius of the well casing, and t_m is the time when matched to the type curve. The numerical slug test data were fitted to Equation (3) in AQTESOLV 4.02. This software package uses a non-linear regression, to fit the type curves of Cooper-Bredehoeft-Papadopoulos's solution (Figure B.5) (Duffield, 2006). The fitting parameters are storativity and transmissivity. The storativity values from the curve fitting are often ignored with the Cooper-Bredehoeft-Papadopoulos method (Fetter, 2001).

The slug test hydraulic conductivity K_{slug} was calculated by dividing T by the thickness of the aquifer. The units for K_{slug} are meters/second. Due to the square shape of the well cell in Processing Modflow 5.30, a value of 0.604m was used as the value for the radius of the well casing (r_c) in Equation 3. This value was determined by setting up 40 homogeneous K fields, each with 59,049 cells containing the same hydraulic conductivity value. A slug test was run in the center of each field. The resulting head response data were then fitted to the Cooper-Bredehoeft-Papadopoulos model and the radius of the well casing was continuously adjusted until the value of K_{slug} exactly matched the value of K_{eff} . This procedure was done over a large range of hydraulic conductivity values to produce a best estimate of r_c . The result of these analyses is a regression equation relating $\ln(K_{slug})$ to $\ln(K_{eff})$ with a slope of ~ 1 , an intercept of ~ 0 and an R^2 value of ~ 1 (Figure B.6).

Once r_c was determined, the Cooper-Bredehoeft-Papadopoulos model was fitted to the head response data from the simulations run in the 40 heterogeneous fields. Table A.1 shows the residual sums of squares for all of these fits.

2.3 Zone of Influence

By examining the zone of influence of the slug test one can detect exactly what extent of the aquifer is being sampled. Every cell with a hydraulic head greater than 10.001m head was used in this measurement (i.e. 0.001m above the initial head value). The zone of influence was determined by examining each of the time steps and looking for the time step with the largest head response around the slugged well. The reason the last time step was not used is because the greatest zone of influence often appeared in the early time steps before full equilibration of the groundwater heads. To measure the zone of influence, the effective length was measured in the x direction (r_x) and y direction (r_y). The measurements were made in the x and y directions to provide a consistent measurement technique for each realization (Figure B.7). These lengths were then normalized with respect to the length of the entire field giving a normalized zone of influence (r_{norm}) ranging from zero to one, in accordance with how much of the aquifer was being sampled (i.e. 0 for when none of the aquifer length was sampled and 1 when all of the aquifer length was sampled).

2.4 Anisotropy

Anisotropy ratios were determined for both the steady-state and the transient simulations. The steady-state anisotropy ratio was determined by examining $K_{x,eff}$ and the $K_{y,eff}$ values (See Section 2.21). These values were expressed as the ratio $K_{x,eff}/K_{y,eff} = \lambda_{eff}$ (anisotropy from the K_{eff} measurements). Next, the length measurements from the transient simulations were analyzed in the x and y directions based on the extent of the zone of influence (See Section 2.4). From this analysis r_x and r_y were determined and an anisotropy ratio was taken as $r_x/r_y = \lambda_r$ (anisotropy from the effective lengths). The purpose of measuring and comparing anisotropy ratios is to see if the values differ for different fields using different measuring techniques between large and small scale tests.

2.5 Statistical Methods

For each p-value (from 1/9 to 8/9), and at the 5 different i scales, 3 random realizations were produced. For example, for p=8/9, i=5 three realizations of the multifractal field were generated and a steady-state simulation and transient simulation were run for each of these realizations. Then for p=8/9, i=4 three realizations were analyzed, so on and so forth, for each p-value and i level. All data can be found in Appendix E. By looking at three realizations for each p-value and scale, one is able to calculate important statistical properties. Due to the fact that the hydraulic conductivities values, often varied by an order of magnitude between realizations the data were ln transformed. Next the averages of the realizations for each specific p and i level of $\ln(K_{eff})$ and $\ln(K_{slug})$ were taken. The untransformed data was not examined.

The statistical analysis that was undertaken in this project included examining the correlation of the data, analysis of variance (ANOVA), comparison of means, and regression analyses. A correlation matrix was built to look for any correlations among the following list of variables: $\ln(K_{eff})$, $\ln(K_{slug})$, λ_{eff} , λ_r , and r_{norm} . For the ANOVA model, the independent effects were p, i, and the interaction between p*i. There were 5 ANOVA models associated with the variables $\ln(K_{eff})$, $\ln(K_{slug})$, λ_{eff} , λ_r , and r_{norm} . If the variables had significant effects for the model, p, i, and/or p*i then an appropriate comparison of means was conducted. Linear regression models were determined between $\ln(K_{slug})$ and $\ln(K_{eff})$ at each i level for the averages of the realizations and all realizations as well as over all p and i levels for all realizations and the averages of the realizations. From each linear regression equation a mean absolute percent error (MAPE) was calculated to determine the percent error in estimation of K_{eff} from K_{slug} . The MAPE was calculated by summing the absolute values of the residuals and dividing by the number of samples.

2.6 Multiple Random Realizations

A specific multifractal field ($p=4/9$, $i=5$, $b=3$) was examined in detail. This was done to compare the results of K_{eff} and K_{slug} for 100 random realizations and the hydraulic conductivity distribution of the 59,049 different K values located in the field (K_{field}). Histograms were constructed based on the relative frequency (expressed as a percentage). This was examined so that K_{field} , with 59,049 values, could be compared to the 100 K_{eff} values and 100 K_{slug} values. The data were \ln transformed and the mean and median were examined for each case. Also statistical tests were run on the data to determine if K_{eff} , K_{slug} , K_{field} , $\ln(K_{\text{eff}})$, $\ln(K_{\text{slug}})$, and $\ln(K_{\text{field}})$ followed normal distributions. The Wilk-Shapiro test for normality at $p<0.05$ was applied to the K_{eff} , K_{slug} , $\ln(K_{\text{eff}})$, and $\ln(K_{\text{slug}})$ values and the Kolomogorov's D test for normality at $p<0.05$ was applied to K_{field} and $\ln(K_{\text{field}})$.

3.0 Results and Discussion

3.1 Detailed Examination of a Specific Multifractal Field

A 2-d multifractal field was examined in detail to determine how the distributions of K_{eff} , K_{slug} , and K_{field} compared. Simulations were run in 100 random realizations of a $p=4/9$, $i=5$, $b=3$ multifractal field. The distribution of the K_{field} values was examined and compared to the K_{slug} and K_{eff} simulation values. Figure B.8 shows that K_{slug} follows a distribution similar to that of K_{field} , largely resulting from small scale sampling. In contrast, K_{eff} samples the entire aquifer resulting in large scale regional hydraulic conductivity values with only a small amount of variation (Figure B.8).

Table A.2 gives the mean, variance, and normality test results for K_{eff} , K_{slug} , K_{field} , $\ln(K_{\text{eff}})$, $\ln(K_{\text{slug}})$, and $\ln(K_{\text{field}})$. The variances for the 100 $\ln(K_{\text{slug}})$ and $\ln(K_{\text{eff}})$ values were 16.65 and 0.41 respectively. The K_{slug} variance is much larger than K_{eff} , because K_{slug} is essentially a point measurement in the aquifer derived from the distribution of hydraulic conductivity values immediately around the well.

All untransformed and \ln transformed measured values were tested for normality. The results show that, in general, all the data sets were closer to a log-normal distribution than a normal distribution. However, only the $\ln(K_{\text{eff}})$ values were not significantly different from a log-normal distribution. This statistical examination of the specific multifractal field shows that working with \ln transformed values is viable. This project initially planned to use log-normal statistics to predict the number of slug tests needed to accurately predict K_{eff} , but since K_{slug} did not statistically follow a log-normal distribution it was not possible to run this test.

3.2 Steady-State Results

The steady-state flow simulations were used in order to determine K_{eff} for each multifractal field. An ANOVA model was constructed where $\ln(K_{\text{eff}})$ is the

dependant variable and p , i , and the interaction between the two terms ($p*i$) were sources of variation. The resulting ANOVA table was used to determine which of these effects were significantly different at $p < 0.05$ (Table A.3). Table A.3 shows that there was significant differences with the effects across all p , i , and $p*i$ levels which was expected since the $\ln(K_{eff})$ values are different for each probability field at each scale. Since there were significant effects across all p , i and $p*i$ the means were split up in order to examine them at the p level associated with their respective i levels. These results were put into a bar graph with corresponding Tukey values associated with each mean (Figure B.9). The bar graph shows that as the p value decreases, $\ln(K_{eff})$ decreases and as i decreases, $\ln(K_{eff})$ increases. These trends were also observed by Koirala et al. (2008).

The variance of $\ln(K_{eff})$ was also determined for each 2-d multifractal field (Table A.4). Notice that the variance tends to increase as the p level decreases, possibly due to lack of connectivity between the cells. Overall the estimations between the different p and i levels had only a small amount of variance considering that only three replications were run for each p and i level. This showed that estimating K_{eff} using the steady-state simulations was fairly consistent. Therefore, the mean $\ln(K_{eff})$ values appear to be a good predictor of the aquifer system for the majority of the p and i levels.

The anisotropy ratio was calculated for all of the multifractal fields using the $K_{eff,x}$ and $K_{eff,y}$ values. This ratio was determined and examined in order to see if there were any significant differences in λ_{eff} due to p , i , and/or $i*p$. The ANOVA showed (Table A.3) that there were no significant effects.

3.3 Slug Test Results

The slug test simulations involved examining the hydraulic head data over time for the center node which was given a 1 meter slug of water. By fitting the data to the Cooper-Bredehoeft-Papadopoulos analytical solution, K_{slug} was determined for each multifractal field. These values were examined in an ANOVA model to determine if there were any significant effects of p , i , and/or $i*p$. The results of the ANOVA table (Table A.3) show that there were significant effects across all levels. Therefore the means were compared by p and i levels with the associated Tukey values (Figure B.10). The means show the same trends as in the steady-state $\ln(K_{eff})$ results, i.e. the means decrease as the p level decreases, and as the i level increases.

The variances for $\ln(K_{slug})$ were determined for the three realizations associated with the corresponding p and i levels (Table A.5). The main trend in this table is seen by p level. As the p level decreases the variance increases. This indicates that a better estimation of $\ln(K_{eff})$ will probably be achieved at the higher p levels or more homogeneous fields. In contrast to the p level, there was no clear trend in the variance when varying the i level/hydrofacies size (Table A.5).

Since the zone of influence (r_{norm}) determines the scale of measurement this variable was also examined to see if there were any significant effects of i , p , and/or $i*p$ (Table A.3). The ANOVA table showed that all three constructed effects were significant. A bar graph was constructed showing the associated Tukey values corresponding to the means by p and i level (Figure B.11). This bar graph shows that a larger portion of the aquifer is being sampled at the higher p values and as the fields decrease from $i=5$ to $i=1$.

Mean values for $\ln(K_{slug})$ and $\ln(r_{norm})$ were then compared over corresponding p and i levels to examine the relationship between the variables. The r_{norm} was \ln

transformed in order to produce a linear relationship. Figure B.12 shows the strong positive relationship between $\ln(K_{slug})$ and $\ln(r_{norm})$. The regression analyses for each i level and over all i levels are summarized in Table A.6. The R^2 value over all i values was 0.85. The R^2 values generally decreased with decreasing i level ($i=5$ having an $R^2=0.98$ and $i=1$ with an $R^2=0.47$). The $i=1$ field was the only one that showed no significant relationship between the variables. This is because a large portion of the aquifer was sampled by the well regardless of the p value. In contrast, at the other i levels, r_{norm} was more dependent on the p value for a given multifractal field.

Given the systematic variation in $\ln(K_{slug})$, apparent in Table A.5, the relationship between r_{norm} and the variance of $\ln(K_{slug})$ was also investigated. Both r_{norm} and the variance of $\ln(K_{slug})$ were \ln transformed in order to produce a linear relationship as shown in Figure B.13. Table A.6 gives the regression results. The overall model R^2 value was 0.35. Examining this trend it is apparent that, as the zone of influence decreases there is more variance in $\ln(K_{slug})$. This suggests that a variation in the $\ln(K_{slug})$ is associated, to some degree, with the amount of the aquifer being sampled. Looking at the regression equations by i level, the R^2 values tended to decrease as the i level decreased (Table A.6). For $i=1$ and $i=2$ there was no significant relationship between the variables. One reason for the large variance observed in the $i=1$ field, even when the zone of influence is large, is because only the middle hydraulic conductivity value of the aquifer is being sampled; therefore the $\ln(K_{slug})$ value tends to this value. As the i level increases more cells are sampled in the model resulting in a lower variance.

The anisotropy ratio of r_{norm} (λ_r) was examined to determine if there were any significant effects due to p , i , and/or $i*p$. The results indicate that there were only significant effects according to i level (Table A.3). Since the model was not significant no further analysis was needed.

3.4 Steady-State and Slug Test Results Compared

3.4.1 Correlations

A correlation matrix for all of the values of $\ln(K_{\text{eff}})$, λ_{eff} , $\ln(K_{\text{slug}})$, r_{norm} , and λ_r was determined (Table A.7). Table A.7 shows the relationships with significant correlations at the $p < 0.01$ level are $\ln(K_{\text{eff}})$ versus $\ln(K_{\text{slug}})$, $\ln(K_{\text{eff}})$ versus r_{norm} , and $\ln(K_{\text{slug}})$ versus r_{norm} . One would expect $\ln(K_{\text{eff}})$ to be correlated with $\ln(K_{\text{slug}})$ since the different estimations of hydraulic conductivity are based on the same fields. The values of $\ln(K_{\text{slug}})$ being correlated with r_{norm} show that at high p values the slug tests sample a larger portion of the aquifer and as the p value decreases so does the fraction of the aquifer being sampled. The values of λ_{eff} and λ_r showed a correlation coefficient of .58 (Table A.7). Since each of the fields were randomly distributed it is no surprise that the anisotropy is different for each ensuing realization. What is interesting is that there is a level of correlation among the small scale measurements of λ_r and the large scale measurements of λ_{eff} . This implication shows that anisotropy at the small (slug test) scale is reflected, to some degree, in the large scale anisotropy of the aquifer effective hydraulic conductivity values, even with two different methods of measurement.

3.4.2 Regression Analyses Over All Replications, p and i Levels

The first regression analysis was run on the 111 values of $\ln(K_{\text{eff}})$ and $\ln(K_{\text{slug}})$ across all p and i levels except for the $p=1/9$, $i=5$, 4, and 3 multifractal fields (omitted because of water balance errors). The R^2 value for the regression was 0.87. The prediction equation, having a high R^2 value, indicates that slug tests are able to measure the effectively hydraulic conductivity accurately over a large range of heterogeneity and hydraulic conductivity. Table A.8 shows the characteristics of this regression equation. The mean absolute percent error (MAPE) demonstrates that the regression equation gives an accurate estimation of $\ln(K_{\text{eff}})$ within 57% of the actual value.

The linear regression, when plotted with the $y=x$ (1:1) line shows that values of $\ln(K_{\text{slug}})$ of the underestimate the true values of $\ln(K_{\text{eff}})$ (Figure B.14). The intersection of $y=x$ and the regression line is at -4.42, -4.42. This demonstrates that the values of $\ln(K_{\text{slug}})$ greater than -4.42 tend to overestimate the true values of $\ln(K_{\text{eff}})$ and that values less than -4.42 underestimate the true value. In low K heterogeneous fields, with pockets of high hydraulic conductivity the values tend to be underestimated and in higher hydraulic conductivity homogenous fields with low K inclusions the values are typically overestimated. The problem with using this equation as a calibration for field estimates is it only accounts for 1 point measurement of hydraulic conductivity. In order to estimate $\ln(K_{\text{eff}})$ more accurately it is important to use replicated measurements of $\ln(K_{\text{slug}})$. Another limitation to the linear regression equation is that all the simulations were run in a 2-d multifractal field neglecting any vertical anisotropy.

3.4.3 Regression Analyses Based on the Averages of Replications Over p and i Levels

Due to the fact that it is common practice to determine aquifer properties from several slugged wells, averages of the three values of $\ln(K_{\text{slug}})$ and $\ln(K_{\text{eff}})$ for each i and p level were computed. From these data a linear regression model was determined for $\ln(K_{\text{slug}})$ versus $\ln(K_{\text{eff}})$. The prediction equation resulting from this analysis is given in Table A.9.

The R^2 value for this regression was 0.96, which is much better than the previous linear regression analysis based on the individual values (Figure B.15). Since the slugged wells were put in the field at random one would expect that, as more of the aquifer is sampled, the averaging of these values would provide a better estimate of $\ln(K_{\text{eff}})$. The intercept of the $x=y$ and the regression line was -3.25, -3.25. This shows that the slug tests in fields with hydraulic conductivities

greater than -3.25 will often overestimate $\ln(K_{\text{eff}})$ of an aquifer, whereas anything less than this value appears to underestimate $\ln(K_{\text{eff}})$.

Median hydraulic conductivity values of the multifractal fields were compared with the K_{eff} values of the field (refer to Table A.10 for median values). Figure B.16 shows that $\ln(K_{\text{eff}})$ overestimates the median field value in low hydraulic conductivity fields and underestimates this value in high hydraulic conductivity fields. This is the same effect we see when K_{slug} estimates K_{eff} . Therefore $\ln(K_{\text{slug}})$ tends to follow the median value of the multifractal field rather than the $\ln(K_{\text{eff}})$ value creating the overestimation and underestimation effect. Some other possible causes for such a large overestimation and underestimation of $\ln(K_{\text{eff}})$ by $\ln(K_{\text{slug}})$ can be related to hydrofacies size and heterogeneity of the aquifer system. For example, with such a large spatial range in the higher resolution/more hydrofacies scale, the slug test encounters more of the lower hydraulic conductivity values within the overall aquifer system based on the random distribution of the K values therefore giving an underestimation of $\ln(K_{\text{eff}})$ by $\ln(K_{\text{slug}})$. Also, flow from the well might be obscured or occluded by hitting a localized string of low K values.

3.4.4 Regression Analyses at Each i Level

To study the scaling effects of K_{slug} and K_{eff} a linear regression analysis was run at each i level over the individual values of $\ln(K_{\text{slug}})$ and $\ln(K_{\text{eff}})$, as well as, the averages of $\ln(K_{\text{slug}})$ and $\ln(K_{\text{eff}})$. The slope, intercept, R^2 , and MAPE were all calculated for each i level (Table A.8, Table A.9). The results show that as the number of hydrofacies in the model increases the MAPE decreases and the R^2 value becomes closer to unity. Consider at the $i=5$ scale there are 59,049 different hydrofacies within that aquifer, while at the $i=1$ scale there is only 9 different hydrofacies. Both of these fields are a 243 by 243 matrix. When a slug

test is administered, the K_{slug} value derived is largely based on the geologic material immediately surrounding the well. Therefore when one is determining $\ln(K_{slug})$ for an $i=1$ field the value is largely influenced by the particular hydraulic conductivity value in the middle of the grid; hence the estimated K_{slug} value is dominated by this one area. Since most of the K values within the $i=1$ grids are larger than K_{eff} (Figure B.16), there is less of a chance that as one inputs a well at random it will hit a block that is less than the K_{eff} .

Examined as a scaling dependency issue, the $i=5$ scale is influenced by a larger number of different hydrofacies than in the $i=1$ case. Often this leads to a better estimation of $\ln(K_{eff})$ by $\ln(K_{slug})$. This can be seen with in the R^2 value for the $i=5$ fields being 0.94 and in contrast to an R^2 value of 0.25 for the $i=1$ fields when all the replications and realizations were examined. The reason for an overestimation at higher p level fields is because r_{norm} is often larger in these higher hydraulic conductivity fields than in the lower hydraulic conductivity fields sampling more values of K in the aquifer (Figure B.11).

When an average of the replications are examined in the model the $i=5$ scale gives an R^2 value of 0.99 while for the $i=1$ scale the $R^2=0.93$. Table A.9 verifies that there is a smaller deviation from the true value when the averages of the three $\ln(K_{slug})$ and $\ln(K_{eff})$ values are used. This can also be seen by comparing the MAPE values over the range of i levels for the average of the three $\ln(K_{slug})$ and $\ln(K_{eff})$ values with the values of all $\ln(K_{slug})$ and $\ln(K_{eff})$ values (Table A.8, Table A.9).

4.0 Conclusions and Further Research

For this project flow simulations were run in 2-d multifractal fields to determine how well K_{slug} estimates K_{eff} for a range of various synthetic aquifer scenarios.

The results showed that overall estimation of K_{eff} by K_{slug} was most accurate when an average value of K_{slug} from three replications was taken. The resulting regression model had an R^2 value of 0.96. These results indicate that slug tests are able to measure, with a large degree of accuracy, the effective hydraulic conductivity of fields over a large range of heterogeneity and K values.

Examining the data in more detail with respect to scale, it is evident that K_{slug} estimates K_{eff} more effectively when there are a range of different hydrofacies in close proximity to one another, i.e. the $i=5$ scale. This is due to the fact that the head response data from the slug test is in essence sampling a larger variety of hydrofacies within the immediate vicinity of the well. Furthermore, fields with less hydrofacies tend to overestimate the effective hydraulic conductivity because the area around the well is predominantly only sampling the center hydraulic conductivity value. In our fields, this cell typically had a higher hydraulic conductivity value in high K fields with low K inclusions than the K_{eff} value. The higher hydraulic conductivity fields also showed an overestimation of K_{eff} by K_{slug} with an underestimation in the low hydraulic conductivity fields with high K inclusions. This is because the K_{slug} tends to follow the median value of the multifractal field which was larger than K_{eff} in high K fields and smaller in low K fields.

In the fields with low hydraulic conductivity and high K inclusions the K_{slug} values that were determined by the slug test tended to have a larger variance than those in the fields of high hydraulic conductivity with low K inclusions. This is largely due to the low hydraulic conductivity fields having hydraulic conductivity values that range over a greater scale than in the higher p values; i.e. they are more heterogeneous.

When using a slug test in the field it is important to use at a minimum an average of three different point measurements. From the analyses conducted here, this average was seen to reduce the error estimation of K_{eff} from 57% to 28%. Two main linear regression equations were developed to predict K_{eff} from slug test data. When used in low hydraulic conductivity multifractal fields the regression equations indicate that K_{slug} is closer to the K_{eff} value, but in high hydraulic conductivity material using the equations will overestimate K_{eff} to some extent. This will help minimize the error associated with well response tests. It is important to remember that the simulations for this project were run in 2-d multifractal fields; therefore these results are limited to only 2-d cases neglecting the vertical component.

The $p=4/9$, $i=5$, $b=3$ multifractal field was a case that was examined in detail. The results showed that the data follows more of a log-normal distribution than a normal distribution. However the only variable that was not statistically different from a normal distribution was $\ln(K_{eff})$. The variance for 100 $\ln(K_{eff})$ values was very small compared to the variance of the 100 $\ln(K_{slug})$ values. This is because the $\ln(K_{eff})$ values sample the entire multifractal field while the $\ln(K_{slug})$ values only samples a small portion of the field.

When implementing a slug test in the field there are several factors that influence the outcome. Therefore it is recommended that common quality assurance programs are set up when conducting a slug test program. This way the field measurement error can be reduced. The present modeling project can help in providing guidelines for interpreting the results from a slug test when extrapolated to the effective hydraulic conductivity of a heterogeneous aquifer system.

To expand this research it might prove valuable to run slug test simulations and steady-state simulations on 3-d multifractal fields. This could be done by extending the models in this project to contain a vertical component. This would better account for what is observed in natural groundwater systems. These results could then be compared to the results from the 2-d multifractal field simulations. It would also be worthwhile to conduct the same type of simulations as in this project on different types of statistically generated hydraulic conductivity fields to see if and how the results are differ to those for the K multifractal fields.

Works Cited

- Babadagli, T., (2006). Effective permeability estimation for 2-D fractal permeability fields. *Mathematical Geology* 38(1): doi: 10.1007/s11004-005-9002-z.
- Boufadel, M. C., Lu, S., Molz, F.J., Lavalle, D., (2000). Multifractal scaling of the intrinsic permeability. *Water Resources Research* 36(11): 3211-3222.
- Bredehoeft, J., (2006). On modeling philosophies. *Ground Water* 44(4): 496-499.
- Butler, J., McElwee, C., Liu, W., (1996). Improving the quality of parameter estimates obtained from slug tests. *Ground Water* 34(3): 480-490.
- Butler, J., Healey, J., (1998). Relationship between pumping-test and slug-test parameters: Scale effect or artifact? *Ground Water* 36(2): 305-313.
- Chapius, R. P., Dallaire V., Marcotte, D., Chouteau, M., Acevedo, N., Gagnon, F., (2005). Evaluating the hydraulic conductivity at three different scales within an unconfined sand aquifer at Lachenaie, Quebec. *Canada Geotech* 42: 1212-1220.
- Chiang, W.-H., Kinzelbach, W., (2001). Processing Modflow Version 5.3.0.
- Cooper, H. H., Bredehoeft, J.D., Papadopoulos, I.S., (1967). Response of a finite-diameter well to an instantaneous charge of water. *Water Resources Research* 3(1): 263-269.

Dreuzy, J. R., Davy, P., Erhel, J., Bremond d' Ars, J., (2004). Anomalous diffusion exponents in continuous two-dimensional multifractal media. *Physical Review* 70: 016306.

Duffield, G. M., (2006). AQTESOLV Version 4.01, HydroSOLVE, Inc.

Eaton, T. T., (2006). On the importance of geological heterogeneity for flow simulation. *Sedimentary Geology*: 184 187-201, doi: 10.1016/j.sedgeo.2005.11.002.

Fetter, C. W., (2001). *Applied Hydrogeology*. Upper Saddle River, New Jersey, Prentice Hall.

Hassan, A. E., Cushman, J.H., Delleur, J.W., (1997). Monte Carlo studies of flow and transport in fractal conductivity fields: Comparison with stochastic perturbation theory. *Water Resources Research* 33(11): 2519-2534.

Koirala, S. R., Perfect, E., Gentry, R.W., Kim, J.W., (2008). Effective saturated hydraulic conductivity of 2-dimensional random multifractal fields. *Water Resources Research*: in press.

Lee, J. Y., Lee, K.K., (1999). Analysis of the quality of parameter estimations from repeated pumping and slug tests in a fractured porous aquifer system in Wonju, Korea. *Ground Water* 37(5): 692-700.

Lenormand, R., Kalaydjian, F., Bieber, M-T., Lombard, J-M., (1990). Use of a multifractal approach for multiphase flow in heterogeneous porous media: comparison with ct-scanning experiment. 65th Annual Technical Conference and Exhibition of the Society of Petroleum Engineers, New Orleans, LA.

- Liu, H. H., Molz, F.J., (1997). Multifractal analyses of hydraulic conductivity distributions. *Water Resources Research* 33(11): 2483-2488.
- Loáiciga, H., A., Yeh, William, W.-G., Ortega-Guerrero, Marcos, Adrián (2006). "Probability Density Functions in the Analysis of Hydraulic Conductivity Data." *Journal of Hydrologic Engineering* **11**(5): 442-450.
- Marsily, G., Delay, F., Teles, V., (1998). Some current methods to represent the heterogeneity of natural media in hydrogeology. *Hydrogeology Journal* 6: 115-130.
- McDonald, M. G., Harbaugh, A.W., (1988). A modular three-dimensional finite-difference groundwater flow model: U.S. Geological Survey Techniques of Water-Resources Investigations. Washington, United States Government Printing Office.
- Molz, F. J., Rajaram, H., Lu, S., (2004). Stochastic fractal-based models of heterogeneity in subsurface hydrology: origins, applications, limitations, and future research questions. *Review of Geophysics*: 42, 1002 doi: 10.1029/2003RG000126.
- Neuman, S. P., Di Federico, V., (2003). Multifaceted nature of hydrogeologic scaling and its interpretation. *Review of Geophysics*: 41, 1014 doi:10.1029/2003RG000130.
- Osiensky, J. L., Williams, R.E., Williams, J., (2000). Evaluation of drawdown curves derived from multiple well aquifer tests in heterogeneous environments. *Mine Water and the Environment* 19(1): 30-55.

- Perfect, E., Gentry, R.W., Sukop, M.C., Lawson, J.E., (2006). Multifractal sierpinski carpets: theory and application to upscaling effective saturated hydraulic conductivity. *Geoderma* 134: 240-252, doi 10.1016/j.geoderma.2006.03.001.
- Renard, P., de Marsily, G., (1997). Calculating equivalent permeability: a review. *Advanced Water Resources*(26): 253-278, 10.1016/S0309-1708(96)00050-4.
- Rovey C., (1998). Digital simulation of the scale effect in hydraulic conductivity. *Hydrogeology Journal* 6: 216-225.
- Rovey, C., Cherkauer, D., (1995). Scale dependency of hydraulic conductivity measurements. *Ground Water* **33**(5): 769-780.
- Rovey, C., Niemann, W., (2001). "Wellskins and slug tests: where's the bias?" *Journal of Hydrology*(243): 120-132.
- Sanchez-Vila, X., Guadagnini, A., Carrera, J., (2006). Representative hydraulic conductivities in saturated groundwater flow. *Review of Geophysics* 44: RG3002, doi:10.1029/2005RG000169.
- Shulze-Makuch, D., Carlson, D., Cherkauer, D., Malik, P., (1999). Scale dependency of hydraulic conductivity in heterogeneous media. *Ground Water* **37**(6): 904-919.
- Tennekoon, L., Boufadel, M.C., (2003). Multifractal anisotropic scaling of the hydraulic conductivity. *Water Resources Research* 39(7): 1193, doi: 10.1029/2002WR001645.

Turcotte, D. L., (1997). *Fractals and Chaos in Geology and Geophysics*,
Cambridge University Press.

Vargas, C., Ortega-Guerrero, A. (2004). Fracture hydraulic conductivity in the
Mexico City clayey aquitard: Field piezometer rising-head tests.
Hydrogeology Journal **12**(3): 336-344.

Veneziano, D., Essiam, A.K., (2003). Flow through porous media with
multifractal hydraulic conductivity. *Water Resources Research* 39(6):
1166, doi: 10.1029/2001WR001019.

Winston, R. B., (2000). Graphical user interface for MODFLOW, Version 4., U.S.
Geological Survey Open-File Report 00-315.

Appendices

Appendix A: Tables

Table A.1 Residual sums of squares for nonlinear fits of head response data in AQTESOLV

P	rep	i				
		5	4	3	2	1
8/9	1	0.00038	0.00017	0.00087	0.00077	0.00074
	2	0.00099	0.00093	0.00027	0.00057	0.00066
	3	0.00088	0.00042	0.00060	0.00053	0.00065
7/9	1	0.00019	0.00175	0.00078	0.00124	0.00053
	2	0.00033	0.00075	0.00157	0.00109	0.04040
	3	0.00475	0.00024	0.00151	0.00026	0.00078
6/9	1	0.00620	0.00302	0.00654	0.00298	0.00058
	2	0.02180	0.00871	0.00159	0.00681	0.03240
	3	0.00738	0.01520	0.00517	0.00364	0.00443
5/9	1	0.00517	0.00565	0.00524	0.01390	0.00228
	2	0.01650	0.01870	0.00295	0.00302	0.00120
	3	0.00058	0.00573	0.00144	0.00613	0.00099
4/9	1	0.00247	0.00004	0.00785	0.01500	0.00094
	2	0.00479	0.00002	0.06100	0.01260	0.00779
	3	0.00361	0.00003	0.06000	0.02850	0.00113
3/9	1	0.00003	0.00247	0.00879	0.00077	0.00040
	2	0.00320	0.00146	0.01750	0.00080	0.01000
	3	0.00624	0.00144	0.00694	0.00089	0.00095
2/9	1	0.00152	0.00008	0.00012	0.21800	0.01190
	2	0.00141	0.00003	0.00641	0.23900	0.00043
	3	0.00154	0.00005	0.00350	0.01210	0.00033
1/9	1	0.00128	0.00313	0.00449	0.00118	0.20400
	2	0.00102	0.03910	0.00901	0.00140	0.01000
	3	0.00120	0.00041	0.00105	0.00128	0.00091

Note: b=3 in every case

Table A.2 Mean, variance, and normality test for the $p=4/9$, $i=5$, $b=3$ multifractal field

	Median	Mean	Variance	Statistic *	Significance
K_{eff}	7.77E-06	8.90E-06	3.03E-11	0.90	<0.0001
K_{slug}	4.13E-06	2.67E-05	3.36E-09	0.51	<0.0001
K_{field}	4.21E-06	7.00E-03	1.60E-03	0.04	<0.01
$\ln(K_{\text{eff}})$	-11.76	-11.82	0.41	0.99	NS
$\ln(K_{\text{slug}})$	-12.40	-13.81	16.65	0.92	<0.0001
$\ln(K_{\text{field}})$	-12.38	-12.83	36.39	0.08	<0.01

*Test for Normality: Kolomogorov's D test used for large number of samples, K_{field} and $\ln(K_{\text{field}})$ at $p<0.05$. Shapiro-Wilk test for small number of samples, K_{eff} , K_{slug} , $\ln(K_{\text{eff}})$, and $\ln(K_{\text{slug}})$ at $p<0.05$. NS: not significantly different at $p<0.05$

Table A.3 ANOVA table significance levels for $\ln(K_{\text{eff}})$, λ_{eff} , $\ln(K_{\text{slug}})$, λ_r , and r_{norm}

	$\ln(K_{\text{eff}})$	$\ln(K_{\text{slug}})$	λ_{eff}	$r_{(\text{norm})}$	λ_r
Model	<0.0001	<0.0001	NS	<0.0001	NS
p	<0.0001	<0.0001	NS	<0.0001	NS
i	<0.0001	<0.0001	NS	<0.0001	0.0238
p*i	<0.0001	<0.0001	NS	0.0004	NS
R²	0.90	0.82	0.35	0.67	0.39

NS: Not significant at $p<0.05$

Table A.4 Variance of $\ln(K_{\text{eff}})$

i	p							
	8/9	7/9	6/9	5/9	4/9	3/9	2/9	1/9
5	0.01>	0.01>	0.01	0.05	0.53	0.21	0.87	ND
4	0.01>	0.01>	0.02	0.08	0.21	1.02	1.25	ND
3	0.01>	0.01>	0.01>	0.01>	0.20	0.10	0.65	ND
2	0.01>	0.01>	0.01>	0.02	0.39	0.03	3.07	1.35
1	0.01>	0.01>	0.01	0.05	0.19	0.06	0.60	1.30

*note cells labled as ND have no values from steady-state

Table A.5 Variance of $\ln(K_{slug})$

i	p							
	8/9	7/9	6/9	5/9	4/9	3/9	2/9	1/9
5	0.01	0.16	0.74	4.12	24.57	11.79	26.86	15.98
4	0.01>	0.15	0.02	1.54	4.51	44.09	89.91	169.55
3	0.37	0.50	0.64	1.81	13.22	9.64	15.28	7.54
2	0.01	2.38	0.02	17.77	18.24	1.88	5.90	25.34
1	0.01>	0.00	1.56	1.47	3.58	8.09	2.72	50.75

Table A.6 Regression models ($y=mx+b$) for the $\ln(\text{mean})$ and $\ln(\text{variance})$ of $\ln(K_{slug})$ versus $\ln(r_{norm})$

	$\ln(\text{mean})$			$\ln(\text{variance})$		
	m	b	R ²	m	b	R ²
All Levels	8.65	0.16	0.85	-1.75	-1.63	0.35
i=5	8.71	-1.58	0.98	-1.21	-1.11	0.53
i=4	8.25	1.62	0.86	-2.73	-4.41	0.87
i=3	10.94	-0.77	0.75	-1.36	-0.24	0.68
i=2	6.58	-0.34	0.87	-2.29	-1.35	0.28*
i=1	2.97	-0.58	0.47*	-7.83	-4.53	0.31*

*Not significant at $p < 0.05$.

Table A.7 Correlation Matrix of $\ln(K_{eff})$, λ_{eff} , $\ln(K_{slug})$, r_{norm} , and λ_r

	$\ln(K_{eff})$	λ_{eff}	$\ln(K_{slug})$	r_{norm}	λ_r
$\ln(K_{eff})$	-	0.37*	0.93**	0.76**	0.07
λ_{eff}	-	-	0.32*	0.20*	0.58*
$\ln(K_{slug})$	-	-	-	0.76**	0.08
r_{norm}	-	-	-	-	0.05
λ_r	-	-	-	-	-

**Represents data that is correlated at $p < 0.01$

*Represents data that is correlated at $p < 0.05$

Table A.8 Linear regression model ($y=mx+b$) showing the slope, intercept, R^2 , MAPE, and the number of observations for each i level for all of the realizations

	m	b	R²	MAPE	Number of observations
All Levels	0.75	-1.11	0.87	57.20%	111
i=5	0.77	-1.10	0.94	25.63%	21
i=4	0.75	-1.12	0.83	36.94%	21
i=3	0.68	-0.93	0.89	43.97%	21
i=2	0.80	-1.19	0.74	69.11%	24
i=1	0.40	-1.69	0.25	119.95%	24

Table A.9 Linear regression model ($y=mx+b$) showing the slope, intercept, R^2 , MAPE, and the number of observations for each i level for an average of the realizations

	m	b	R²	MAPE	Number of observations
All Levels	0.83	-0.56	0.96	28.00%	37
i=5	0.81	-0.60	0.99	9.49%	7
i=4	0.90	0.26	0.97	20.60%	7
i=3	0.74	-0.54	0.96	26.80%	7
i=2	0.97	-0.32	0.88	34.80%	8
i=1	1.42	0.19	0.93	48.04%	8

Table A.10 In transformed median values for the multifractal fields

		p						
l	8/9	7/9	6/9	5/9	4/9	3/9	2/9	1/9
5	-0.76	-2.45	-4.58	-7.74	-12.38	-18.78	-28.13	ND
4	-0.48	-1.71	-3.61	-6.26	-9.86	-14.89	-22.30	ND
3	-0.39	-1.20	-2.44	-4.42	-7.17	-11.18	-16.68	ND
2	-0.76	-0.52	-1.28	-2.47	-4.21	-6.77	-10.85	-16.89
1	0.00	-0.06	-0.27	-0.72	-1.50	-2.69	-4.48	-7.49

*note cells labeled as ND were not determined

Appendix B: Figures

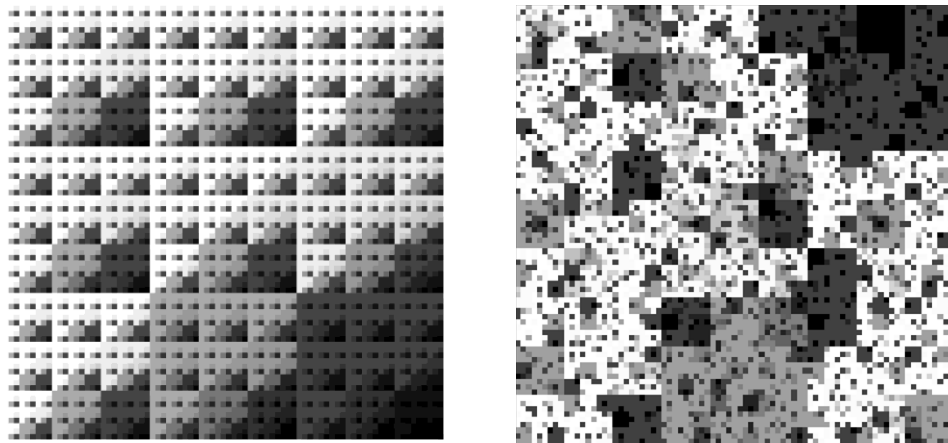


Figure B.1 Deterministic 2-dimensional multifractal field for $p=8/9$, $i=5$, $b=3$ (left) and random 2-dimensional multifractal field for $p=8/9$, $i=5$, $b=3$ (right)

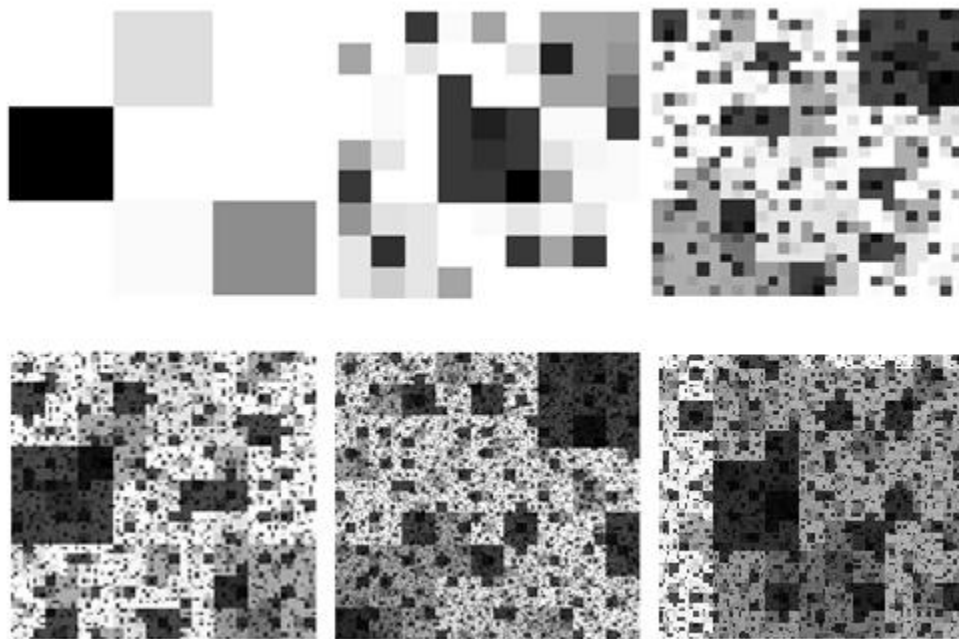


Figure B.2 Six different scales for a $p=8/9$, $b=3$ random 2-d multifractal field. From top left to bottom right: $i=1$, $i=2$, $i=3$, $i=4$, $i=5$, $i=6$. Black cells: low K , white cells: high K

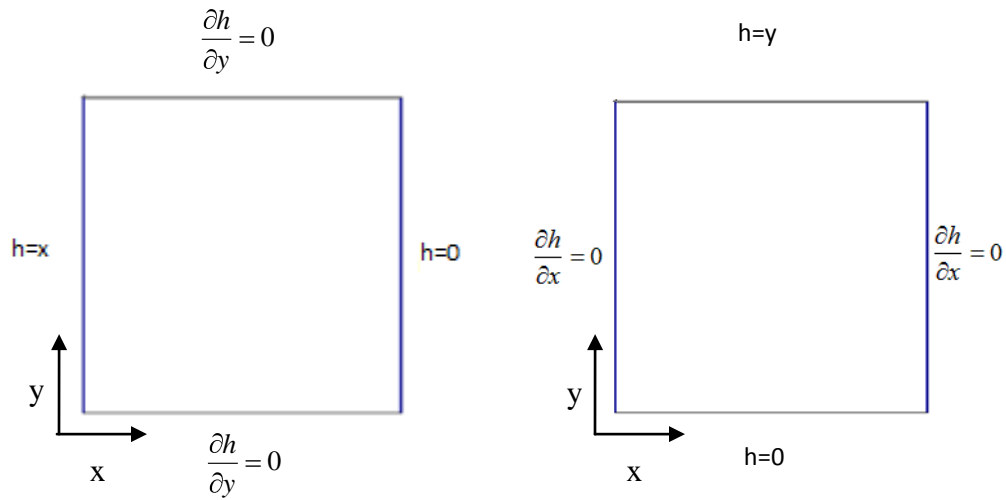


Figure B.3 Boundary conditions for the steady-state flow simulations. Steady-state flow in the x direction (left) steady-state flow in the y direction (right)

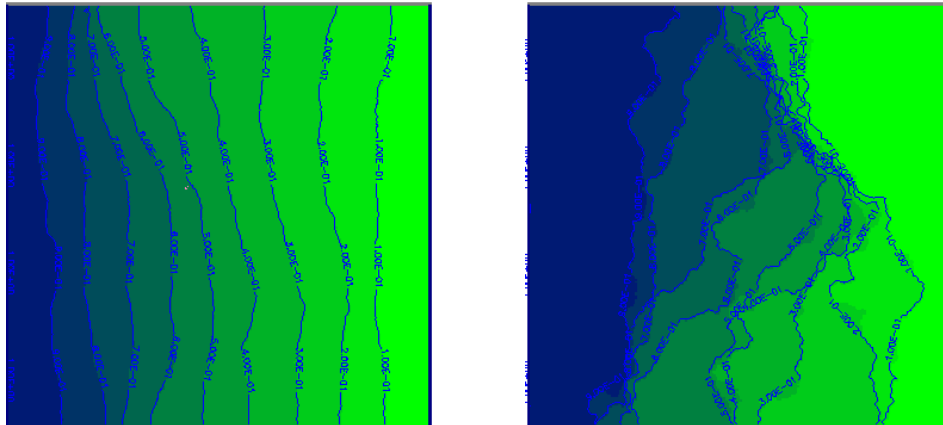


Figure B.4 Example head distributions with contour intervals of 0.1 for steady-state flow in the x direction for random 2-d multifractal fields: $p=8/9$, $i=5$, $b=3$ (left) and $p=5/9$, $i=5$, $b=3$ (right)

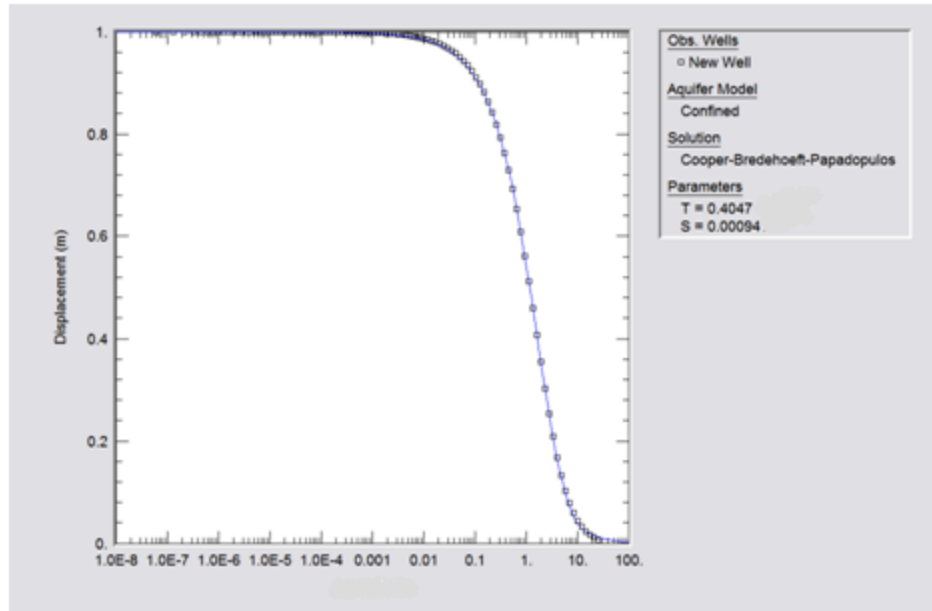


Figure B.5 Example AQTESOLV non-linear regression fit for head response data

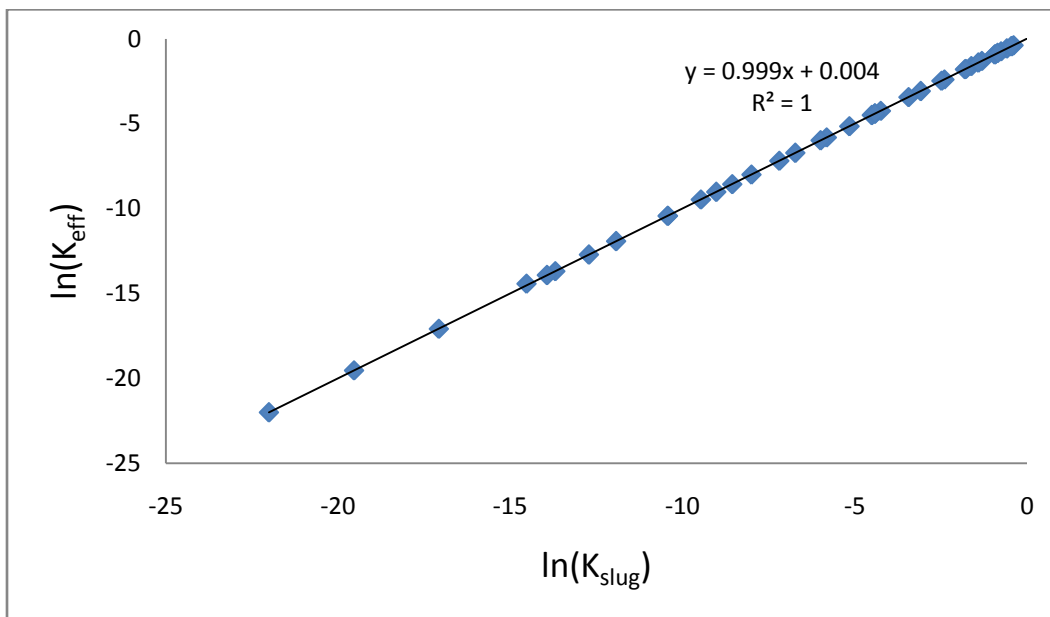


Figure B.6 Relationship between $\ln(K_{eff})$ and $\ln(K_{slug})$ with r_c optimized for 40 homogeneous fields

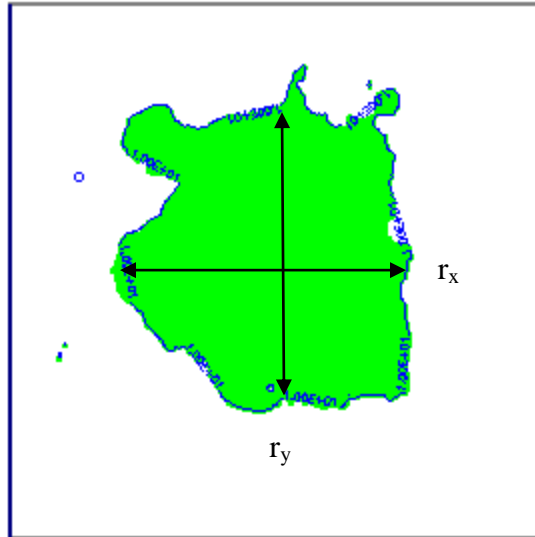


Figure B.7 Measurement of the zone of influence in the x and y directions for the transient slug test simulations

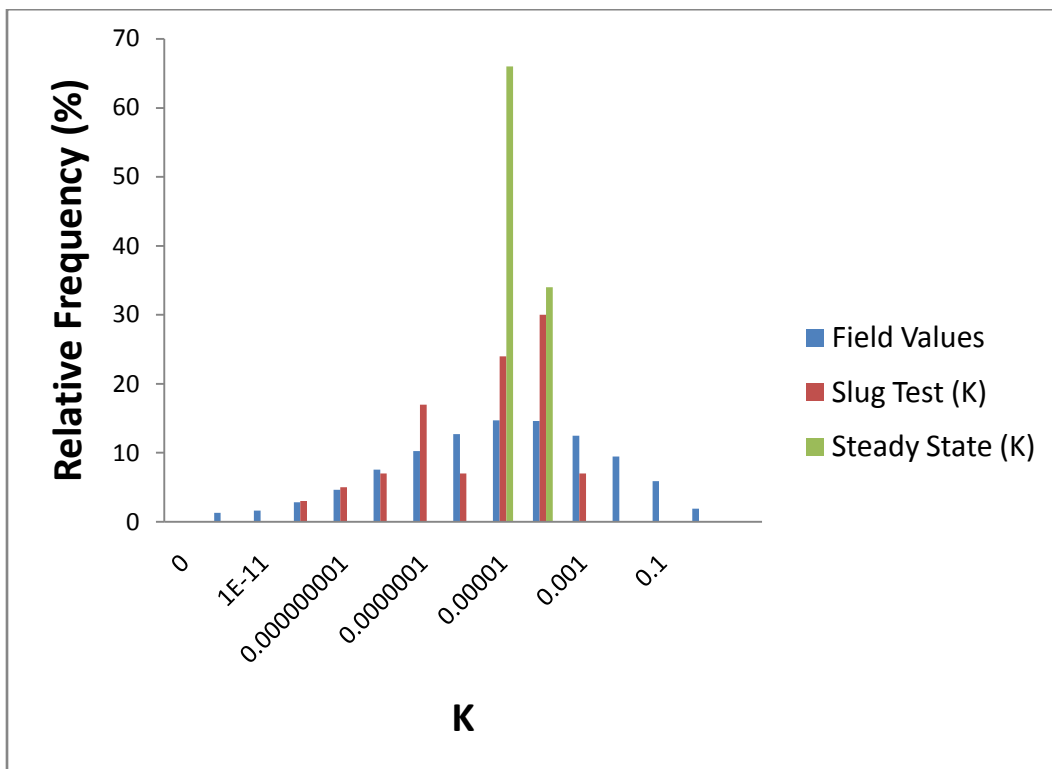


Figure B.8 Histograms of 100 realizations of K_{eff} and K_{slug} and 59,049 K field values for the $p=4/9$, $i=5$, $b=3$ multifractal field

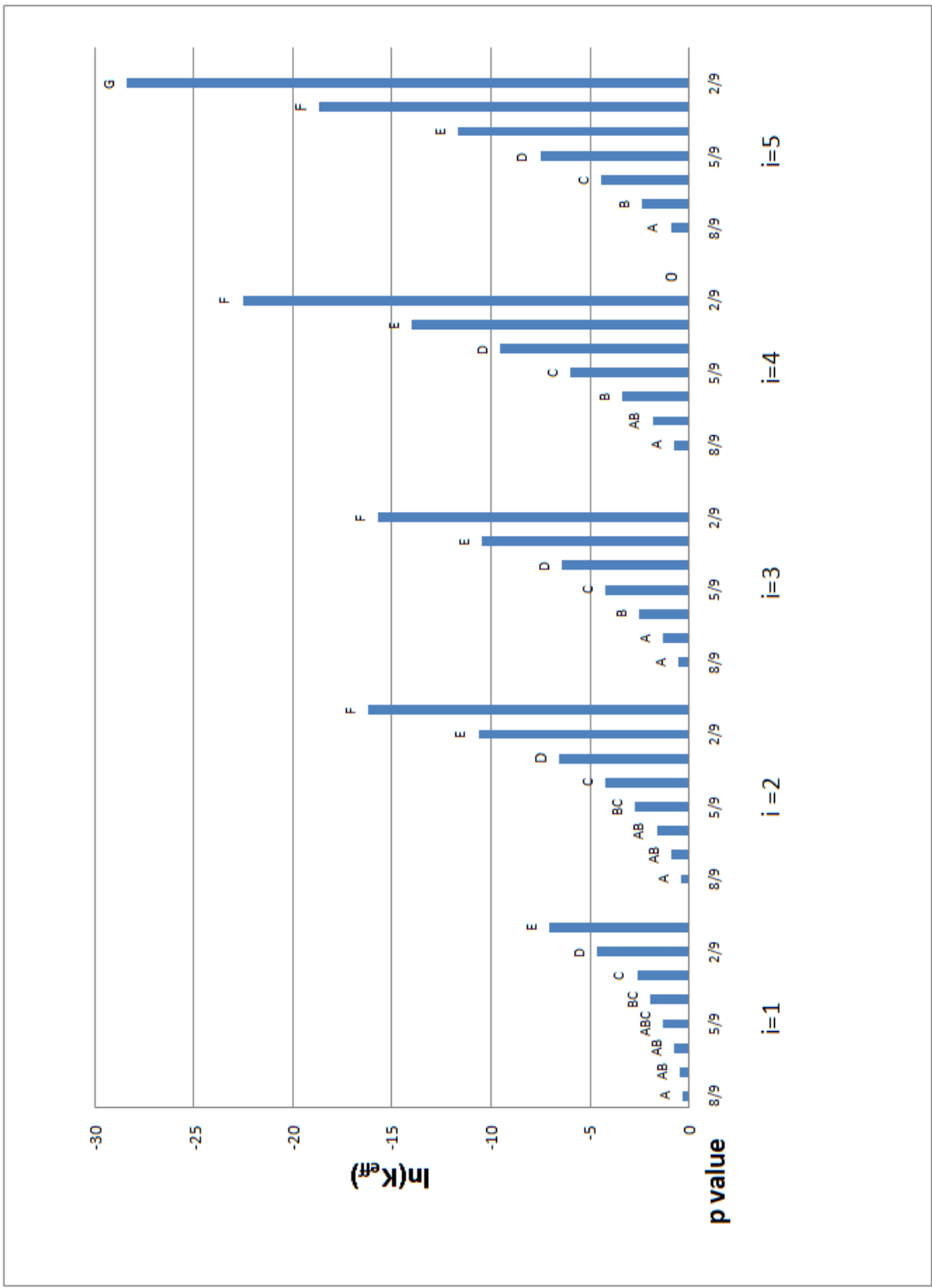


Figure B.9 Mean values for K_{eff} with associated Tukey values by i level. Means with the same letter, within an i -level, are not significantly different at $p < 0.05$

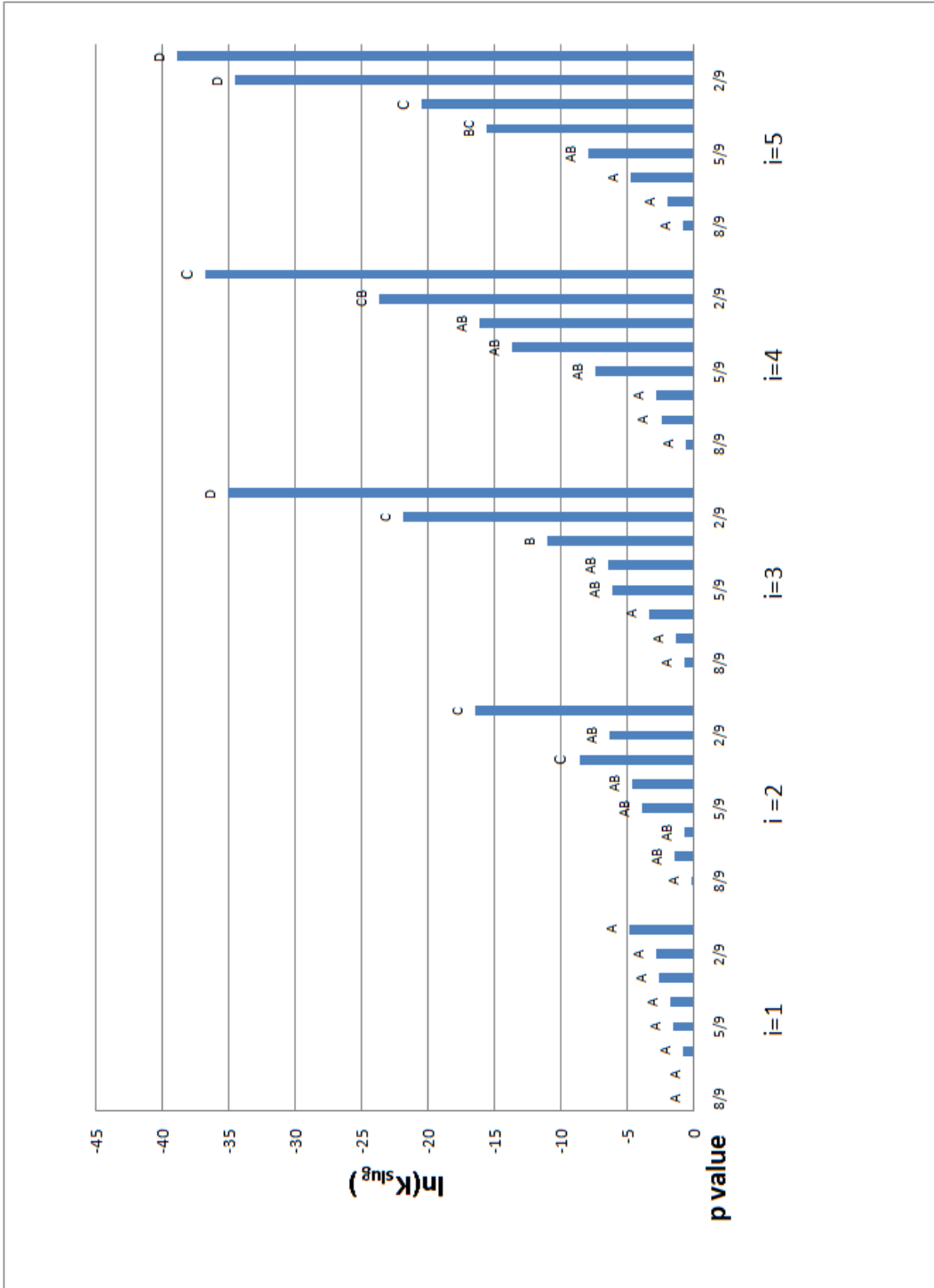


Figure B.10 Mean values for K_{slug} with associated Tukey values by i level. Means with the same letter, within an i-level, are not significantly different at $p < 0.05$

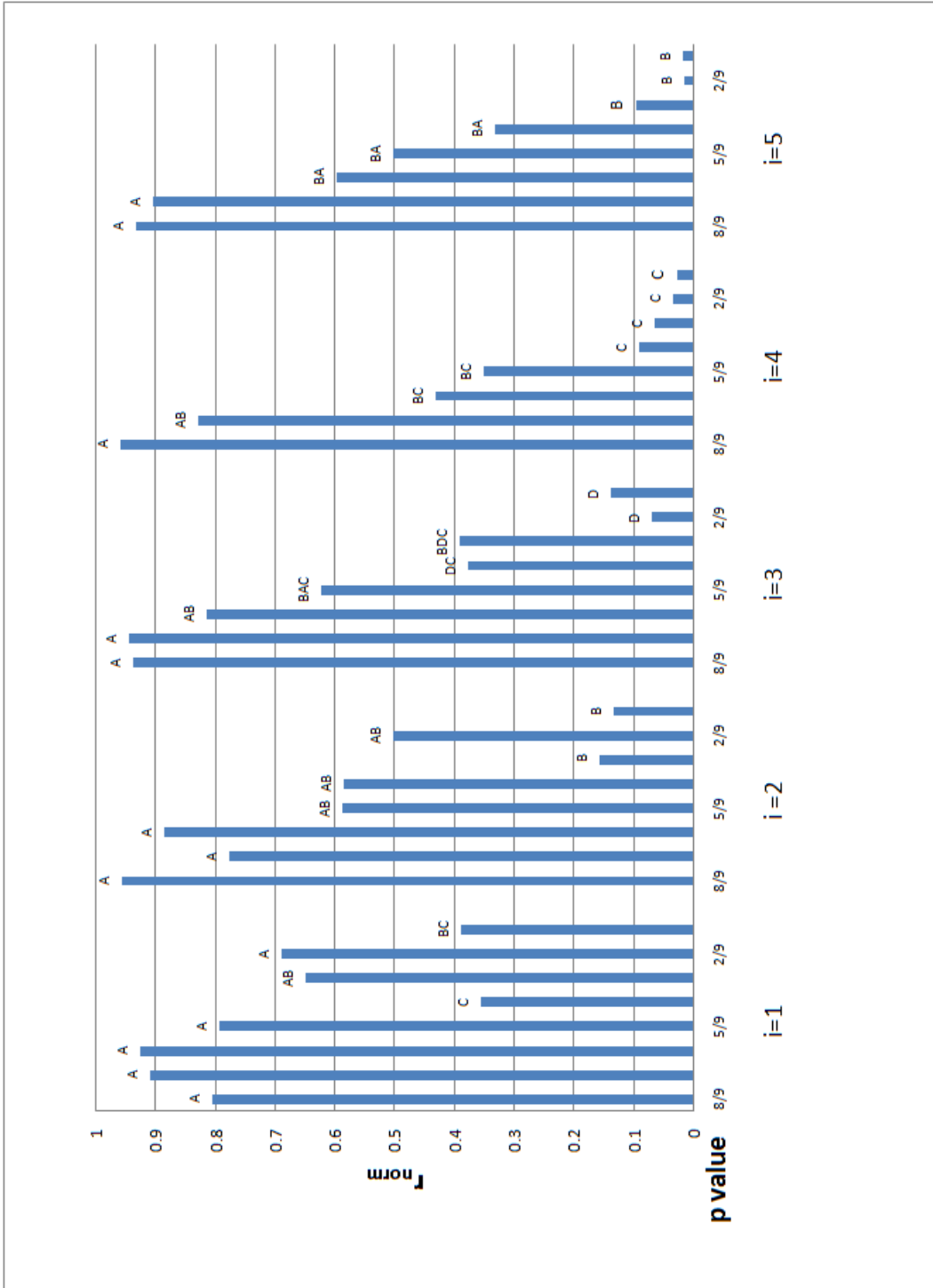
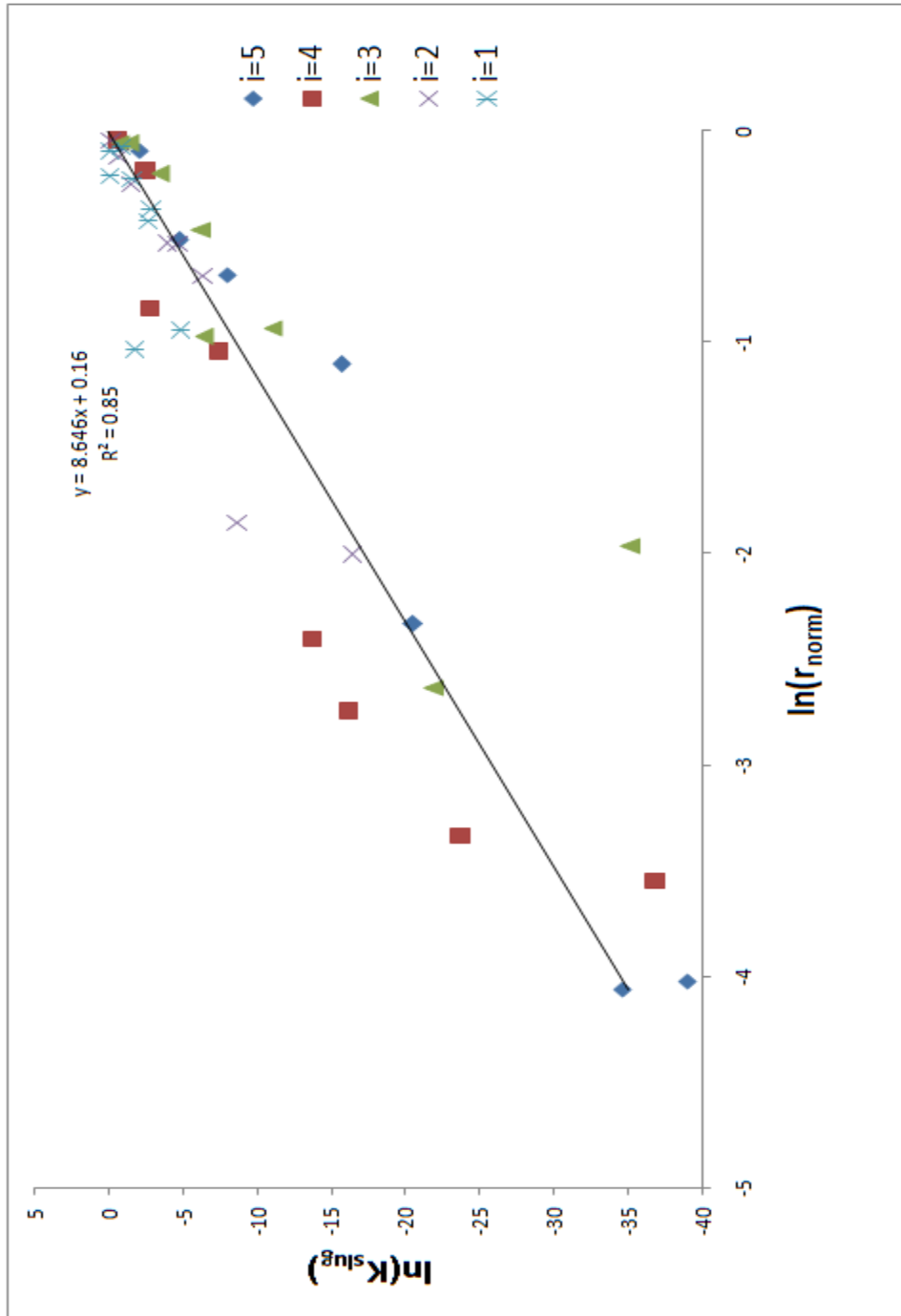


Figure B.11 Mean values for r_{norm} associated with the transient simulations and with associated Tukey values by i level. Means with the same letter, within an i level are not significantly different at $p < 0.05$



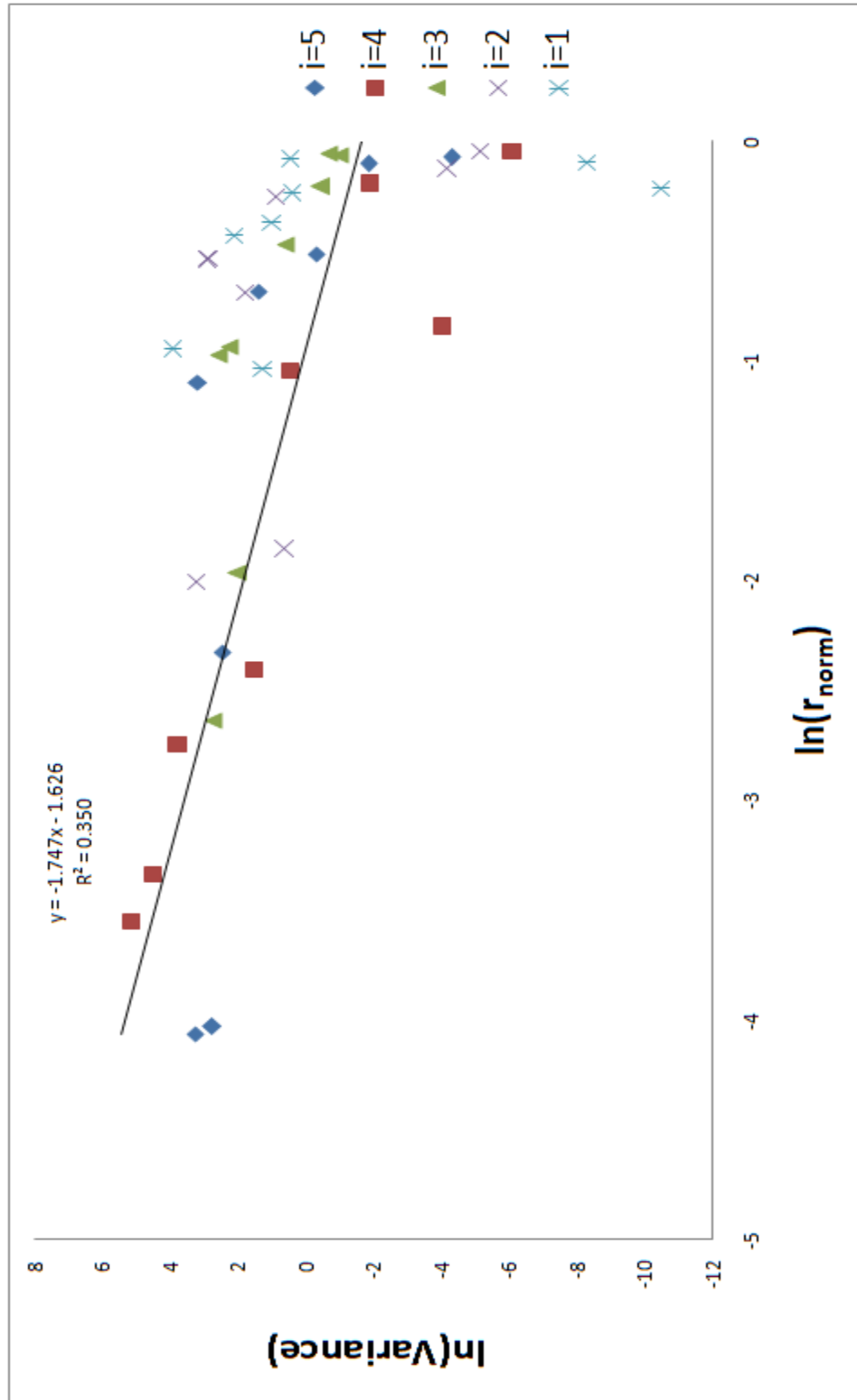


Figure B.13 Plot of the ln transformed variance of $\ln(K_{\text{slug}})$ versus $\ln(r_{\text{norm}})$

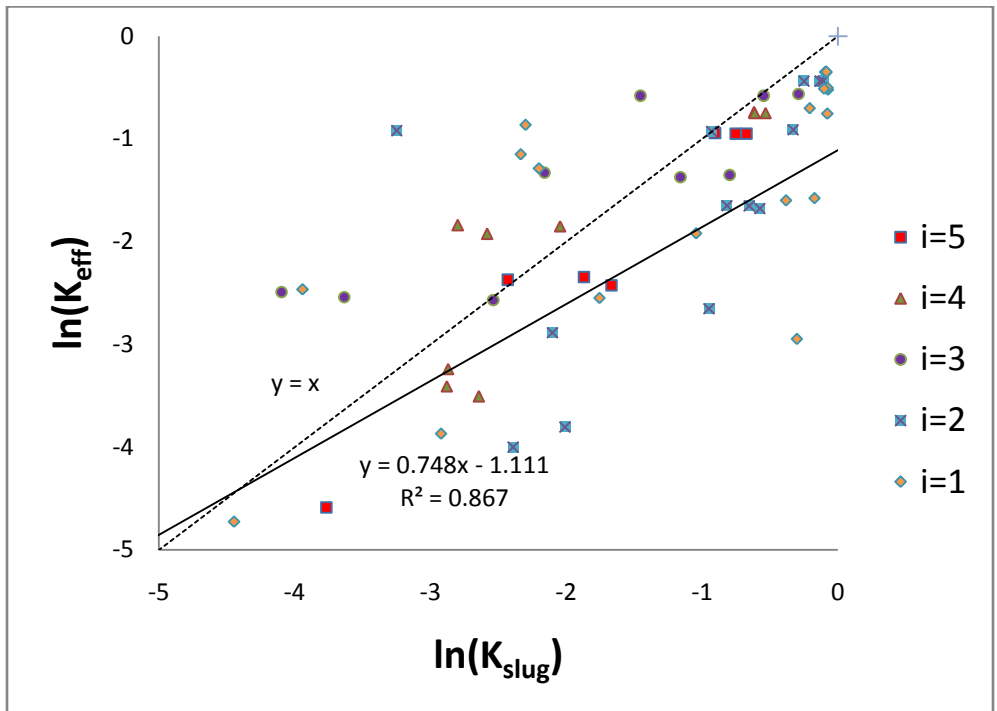
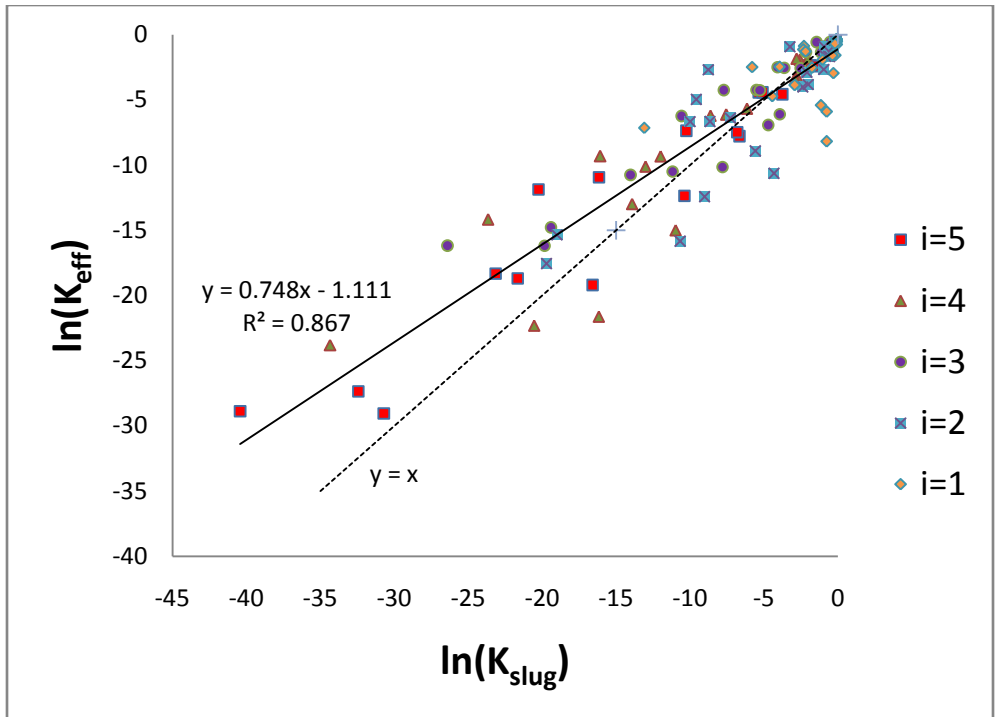


Figure B.14 Linear regression plots for all realizations with the 1 to 1 line(Top).Magnification of the linear regression plot from (-5,-5) (Bottom)

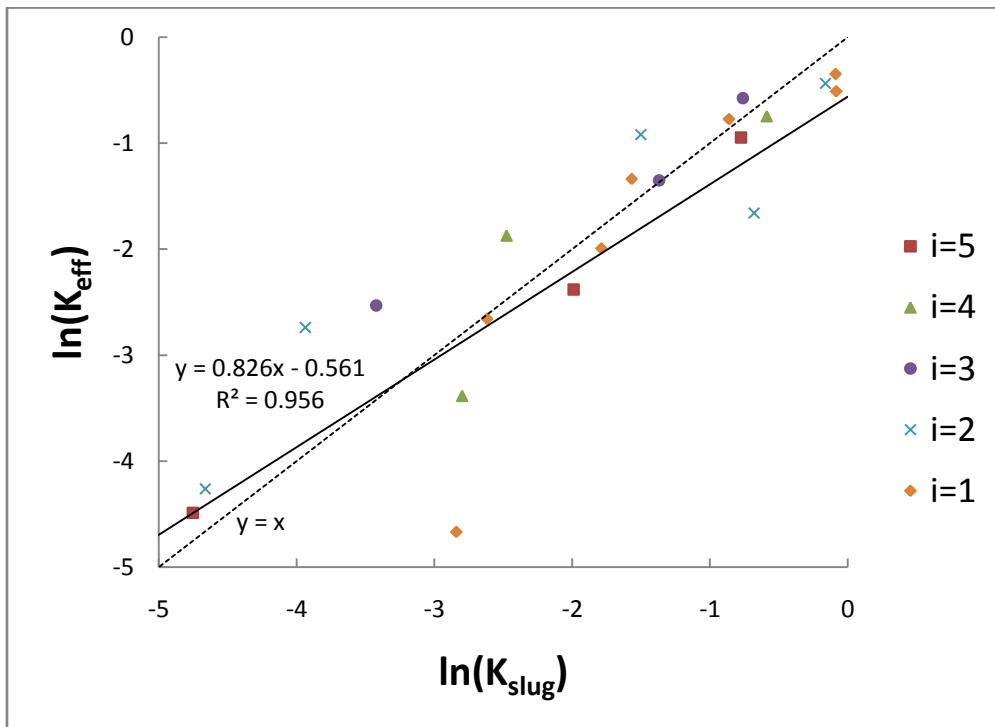
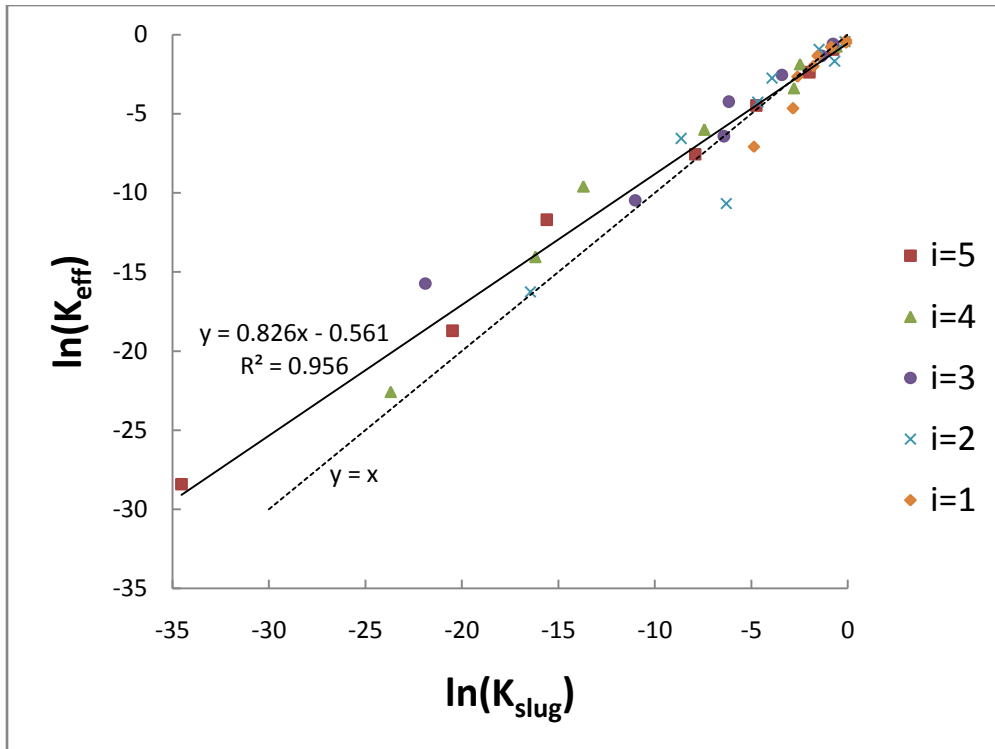


Figure B.15 Linear regression plots for an average of the realizations with the 1 to 1 line (Top). Magnification of the linear regression plot from (-5,-5) (Bottom)

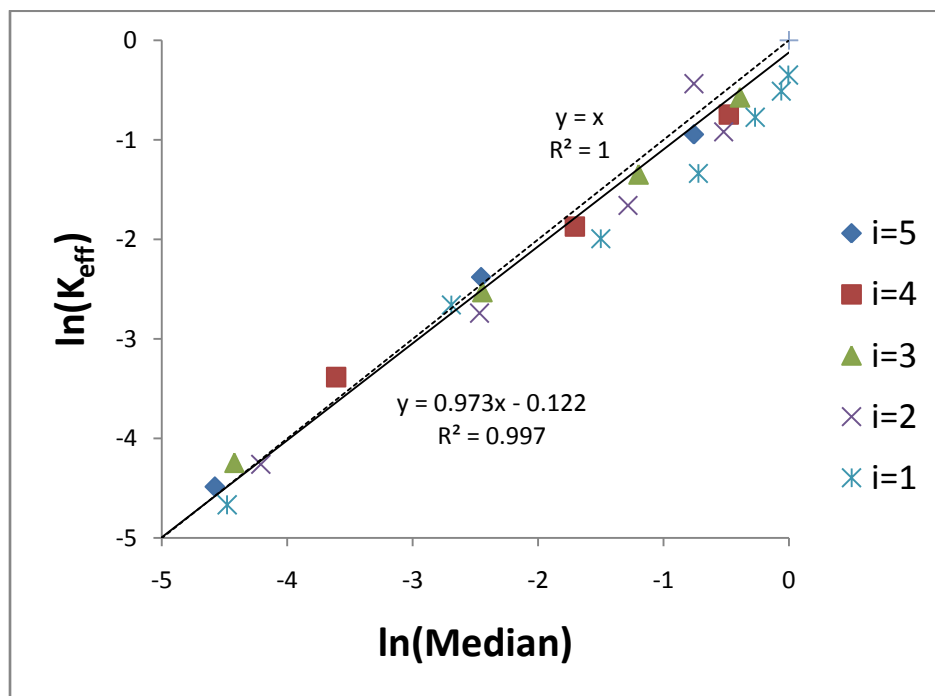
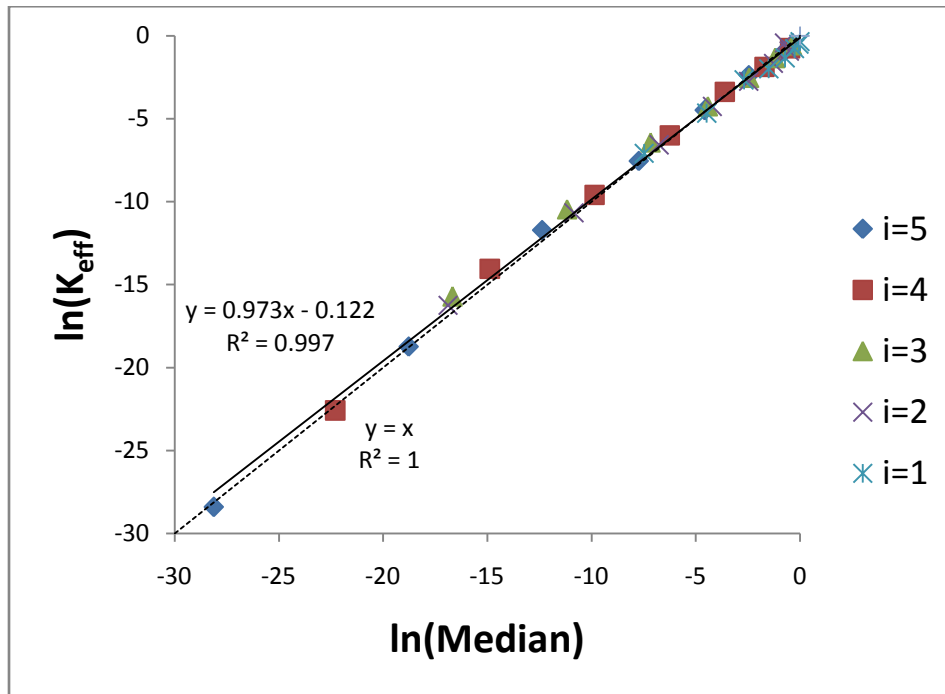


Figure B.16 Linear regression plots for an average of the realizations $\ln(K_{\text{eff}})$ values with the corresponding $\ln(\text{Median})$ values with the 1 to 1 line (Top). Magnification of the linear regression plot from $(-5, -5)$ (Bottom)

Appendix C: Modified MATLAB code

Original Code i=5

```
% Multifractal
% OUTPUT : image of multifractal
%      multifractal.dat file of multifractal

clear all;

disp(' ');
disp('*****');
b = input('Scale factor (default = 3) [Integer] ... ');
maxit = input('Iteration number (default = 3) [Integer] ... ');
pb = input('Numerator of probability (default = 8) [Integer] ... ');

if isempty(b) == 1
    b = 3;
end
if isempty(maxit) == 1
    maxit = 3;
end
if isempty(pb) == 1
    pb = 8;
end

n = b^2; % total number
p = pb/n; % probability

% binomial distribution
for k = 1:n
    bidi(k) = binopdf(n-k+1,n,p);
end

% truncated binomial distribution
tbidi = bidi/sum(bidi);

% average mass fraction in multifractal
f(1) = tbidi(1)/n;
for k = 2:n
    f(k) = f(k-1)+tbidi(k)/(n-k+1);
end

% deterministic or random
disp(' ');
disp('*****');
disp('1. Random multifractal (default)');
disp('2. Deterministic multifractal');
dor = input('Choose type of generator ... ');
if isempty(dor) == 1
    dor = 1;
elseif dor ~= 1 & dor ~= 2
```



```

disp('!!!! Wrong selection ... Try it again ... !!!!!');
return
end

if dor == 2 % deterministic location (using progression)
genn = input('Matrix of generator ... ');
if isempty(genn) == 1
for i = 1:b
for j = 1:b
lgen(b-i+1,j) = (1+(i-1)*(i+2)/2) + (j+(i-1)*2)*(j-1)/2;
ugen(i,b-j+1) = (b^2-(i-1)*(i+2)/2) - (j+(i-1)*2)*(j-1)/2;
end
end
genn = tril(lgen,-1)+triu(ugen);
elseif size(genn) ~= [b b]
disp('!!!! Wrong Generator Input ... Try it again ... !!!!!');
return
end

for i = 1:b
for j = 1:b;
gen(i,j) = f(genn(i,j));
end
end
end

% multifractal
matold = 1;
for it = 1:maxit

[nrow ncol] = size(matold);
matnew = zeros(nrow,ncol);
for i = 1:nrow
for j = 1:ncol

if dor == 1 % random location
rndf = randperm(n);
for ii = 1:b
for jj = 1:b
gen(ii,jj) = f(rndf((ii-1)*b+jj));
end
end
end

matnew((i-1)*b+1:i*b,(j-1)*b+1:j*b) = matold(i,j)*gen;
end
end
matold = matnew
end

% normaize
mat = (matold - min(min(matold))*ones(size(matold))) ...
/ (max(max(matold)) - min(min(matold)));

```

```

A=mat

% data file output
save multifractal.dat A -ascii;

% visualization;
[nrow,ncol] = size(mat);
face = [];
vertex = [];
tcolor = [];
countr = 1;
for i = 1:nrow
    for j = 1:ncol
        xmin = (j-1)/ncol;
        xmax = j/ncol;
        ymin = (i-1)/nrow;
        ymax = i/nrow;
        vertex = [vertex; [xmin ymin 1;xmin ymax 1;xmax ymax 1;xmax ymin 1]];
        face = [face; [countr*4-3 countr*4-2 countr*4-1 countr*4]];
        tcolor = [tcolor; mat(i,j)];
        countr = countr+1;
    end
end
figure
patch('faces',face,'vertices',vertex,'FaceVertexCData',tcolor,'FaceColor','flat',...
'LineStyle','none');
axis([0 1 0 1]);
set(gca,'Box','on','Position',[0 0 1 1]);
set(gcf, 'NumberTitle','off','Name','Multifractal','pos',[200 100 500 500]);
colormap(gray);

```

Modifications to Original Code

i=4

```

A=cell2mat( cellfun(@(v) repmat(v,3,3), ...
mat2cell(mat,repmat(1,1,size(mat,1)),repmat(1,1,size(mat,2))), ...
'UniformOutput', 0) )

```

i=3

```

A=cell2mat( cellfun(@(v) repmat(v,9,9), ...
mat2cell(mat,repmat(1,1,size(mat,1)),repmat(1,1,size(mat,2))), ...
'UniformOutput', 0) )

```

i=2

```

A=cell2mat( cellfun(@(v) repmat(v,27,27), ...
mat2cell(mat,repmat(1,1,size(mat,1)),repmat(1,1,size(mat,2))), ...
'UniformOutput', 0) )

```

i=1

```
A=cell2mat( cellfun(@(v) repmat(v,81,81), ...  
mat2cell(mat,repmat(1,1,size(mat,1)),repmat(1,1,size(mat,2))), ...  
'UniformOutput', 0) )
```

Appendix D: Water budget errors >0.05% for transient simulations

p=3/9, i=5 realization 2

VOLUMETRIC BUDGET FOR ENTIRE MODEL AT END OF TIME STEP 50 IN STRESS PERIOD 1

0	CUMULATIVE VOLUMES	L**3	RATES FOR THIS TIME STEP	L**3/T
	IN:		IN:	
	---		---	
	STORAGE = 1.0003		STORAGE = 0.23452E-14	
	CONSTANT HEAD = 0.84418E-02		CONSTANT HEAD = 0.98416E-13	
0	TOTAL IN = 1.0088		TOTAL IN = 0.10076E-12	
0	OUT:		OUT:	
	---		---	
	STORAGE = 0.48481E-03		STORAGE = 0.37435E-15	
	CONSTANT HEAD = 0.73697E-02		CONSTANT HEAD = 0.12978E-12	
0	TOTAL OUT = 0.78545E-02		TOTAL OUT = 0.13015E-12	
0	IN - OUT = 1.0009		IN - OUT = -0.29389E-13	
0	PERCENT DISCREPANCY =	196.91	PERCENT DISCREPANCY =	-25.45

p=3/9, i=5, realization 3

VOLUMETRIC BUDGET FOR ENTIRE MODEL AT END OF TIME STEP 50 IN STRESS PERIOD 1

0	CUMULATIVE VOLUMES	L**3	RATES FOR THIS TIME STEP	L**3/T
	IN:		IN:	
	---		---	
	STORAGE = 0.99963		STORAGE = 0.14548E-11	
	CONSTANT HEAD = 0.91690E-03		CONSTANT HEAD = 0.21803E-15	
0	TOTAL IN = 1.0005		TOTAL IN = 0.14551E-11	
0	OUT:		OUT:	
	---		---	
	STORAGE = 0.39428E-01		STORAGE = 0.72954E-15	
	CONSTANT HEAD = 0.19047E-02		CONSTANT HEAD = 0.20080E-13	
0	TOTAL OUT = 0.41333E-01		TOTAL OUT = 0.20809E-13	
0	IN - OUT = 0.95921		IN - OUT = 0.14343E-11	
0	PERCENT DISCREPANCY =	184.13	PERCENT DISCREPANCY =	194.36

p=3/9, i=4, realization 2

VOLUMETRIC BUDGET FOR ENTIRE MODEL AT END OF TIME STEP100 IN STRESS PERIOD 1

0	CUMULATIVE VOLUMES	L**3	RATES FOR THIS TIME STEP	L**3/T	
IN:		IN:			
---		---			
STORAGE =	1.0103		STORAGE =	0.23331E-08	
CONSTANT HEAD =	0.22043E-04		CONSTANT HEAD =	0.14397E-12	
0	TOTAL IN = 1.0103		0	TOTAL IN = 0.23332E-08	
0	OUT:		0	OUT:	
----		----			
STORAGE =	0.50884E-01		STORAGE =	0.81211E-10	
CONSTANT HEAD =	0.18455		CONSTANT HEAD =	0.13564E-07	
0	TOTAL OUT = 0.23544		0	TOTAL OUT = 0.13645E-07	
0	IN - OUT = 0.77487		0	IN - OUT = -0.11312E-07	
0	PERCENT DISCREPANCY =	124.40	0	PERCENT DISCREPANCY =	-141.59

p=3/9, i=4, realization 3

VOLUMETRIC BUDGET FOR ENTIRE MODEL AT END OF TIME STEP100 IN STRESS PERIOD 1

0	CUMULATIVE VOLUMES	L**3	RATES FOR THIS TIME STEP	L**3/T	
IN:		IN:			
---		---			
STORAGE =	1.0039		STORAGE =	0.11523E-10	
CONSTANT HEAD =	0.58413E-04		CONSTANT HEAD =	0.94318E-12	
0	TOTAL IN = 1.0040		0	TOTAL IN = 0.12466E-10	
0	OUT:		0	OUT:	
----		----			
STORAGE =	0.82291E-01		STORAGE =	0.91526E-10	
CONSTANT HEAD =	0.14926		CONSTANT HEAD =	0.10978E-07	
0	TOTAL OUT = 0.23155		0	TOTAL OUT = 0.11069E-07	
0	IN - OUT = 0.77244		0	IN - OUT = -0.11057E-07	
0	PERCENT DISCREPANCY =	125.04	0	PERCENT DISCREPANCY =	-199.55

p=3/9, i=3, realization 2

VOLUMETRIC BUDGET FOR ENTIRE MODEL AT END OF TIME STEP100 IN STRESS PERIOD 1

0	CUMULATIVE VOLUMES	L**3	RATES FOR THIS TIME STEP	L**3/T	
IN:		IN:			
---		---			
STORAGE =	2.3621		STORAGE =	0.15142E-05	
CONSTANT HEAD =	0.39834E-04		CONSTANT HEAD =	0.19239E-11	
0	TOTAL IN = 2.3621		0	TOTAL IN = 0.15142E-05	
0	OUT:		0	OUT:	
----		----			
STORAGE =	1.5050		STORAGE =	0.41096E-07	
CONSTANT HEAD =	0.96319		CONSTANT HEAD =	0.21268E-05	
0	TOTAL OUT = 2.4682		0	TOTAL OUT = 0.21679E-05	
0	IN - OUT = -0.10611		0	IN - OUT = -0.65376E-06	
0	PERCENT DISCREPANCY =	-4.39	0	PERCENT DISCREPANCY =	-35.51

p=3/9, i=3, realization 3

VOLUMETRIC BUDGET FOR ENTIRE MODEL AT END OF TIME STEP100 IN STRESS PERIOD 1

0	CUMULATIVE VOLUMES	L**3	RATES FOR THIS TIME STEP	L**3/T	
IN:		IN:			
---		---			
STORAGE =	1.6229		STORAGE =	0.17742E-05	
CONSTANT HEAD =	0.22154E-04		CONSTANT HEAD =	0.22757E-09	
0	TOTAL IN = 1.6230		0	TOTAL IN = 0.17744E-05	
0	OUT:		0	OUT:	
----		----			
STORAGE =	0.75179		STORAGE =	0.29253E-07	
CONSTANT HEAD =	0.89988		CONSTANT HEAD =	0.20187E-05	
0	TOTAL OUT = 1.6517		0	TOTAL OUT = 0.20479E-05	
0	IN - OUT = -0.28703E-01		0	IN - OUT = -0.27352E-06	
0	PERCENT DISCREPANCY =	-1.75	0	PERCENT DISCREPANCY =	-14.31

p=2/9, i=5, realization 1

VOLUMETRIC BUDGET FOR ENTIRE MODEL AT END OF TIME STEP 50 IN STRESS PERIOD 1

0	CUMULATIVE VOLUMES	L**3	RATES FOR THIS TIME STEP	L**3/T	
IN:		IN:			
---		---			
STORAGE =	1.0015		STORAGE =	0.10763E-16	
CONSTANT HEAD =	0.77793E-03		CONSTANT HEAD =	0.16903E-17	
0	TOTAL IN = 1.0023		0	TOTAL IN = 0.12453E-16	
0	OUT:		0	OUT:	
----		----			
STORAGE =	0.20399E-02		STORAGE =	0.48289E-20	
CONSTANT HEAD =	0.29365E-03		CONSTANT HEAD =	0.10956E-18	
0	TOTAL OUT = 0.23335E-02		0	TOTAL OUT = 0.11439E-18	
0	IN - OUT = 0.99999		0	IN - OUT = 0.12339E-16	
0	PERCENT DISCREPANCY =	199.07	0	PERCENT DISCREPANCY =	196.36

p=2/9, i=5, realization 2

VOLUMETRIC BUDGET FOR ENTIRE MODEL AT END OF TIME STEP100 IN STRESS PERIOD 1

0	CUMULATIVE VOLUMES	L**3	RATES FOR THIS TIME STEP	L**3/T	
IN:		IN:			
---		---			
STORAGE =	0.99946		STORAGE =	0.36271E-20	
CONSTANT HEAD =	8.0098		CONSTANT HEAD =	0.31062E-18	
0	TOTAL IN = 9.0093		0	TOTAL IN = 0.31424E-18	
0	OUT:		0	OUT:	
----		----			
STORAGE =	0.23648E-02		STORAGE =	0.14305E-25	
CONSTANT HEAD =	5.7748		CONSTANT HEAD =	0.47020E-19	
0	TOTAL OUT = 5.7772		0	TOTAL OUT = 0.47020E-19	
0	IN - OUT = 3.2321		0	IN - OUT = 0.26722E-18	
0	PERCENT DISCREPANCY =	43.72	0	PERCENT DISCREPANCY =	147.94

p=2/9, i=5, realization 3

VOLUMETRIC BUDGET FOR ENTIRE MODEL AT END OF TIME STEP100 IN STRESS PERIOD 1

0	CUMULATIVE VOLUMES	L**3	RATES FOR THIS TIME STEP	L**3/T	
IN:		IN:			
---		---			
STORAGE =	0.99624		STORAGE =	0.84961E-20	
CONSTANT HEAD =	0.73170		CONSTANT HEAD =	0.63212E-16	
0	TOTAL IN = 1.7279		0	TOTAL IN = 0.63220E-16	
0	OUT:		0	OUT:	
----		----			
STORAGE =	0.22658E-02		STORAGE =	0.44413E-19	
CONSTANT HEAD =	0.60419		CONSTANT HEAD =	0.84521E-16	
0	TOTAL OUT = 0.60646		0	TOTAL OUT = 0.84566E-16	
0	IN - OUT = 1.1215		0	IN - OUT = -0.21345E-16	
0	PERCENT DISCREPANCY =	96.08	0	PERCENT DISCREPANCY =	-28.89

p=2/9, i=4, realization 1

VOLUMETRIC BUDGET FOR ENTIRE MODEL AT END OF TIME STEP 50 IN STRESS PERIOD 1

0	CUMULATIVE VOLUMES	L**3	RATES FOR THIS TIME STEP	L**3/T	
IN:		IN:			
---		---			
STORAGE =	0.99266		STORAGE =	0.12021E-10	
CONSTANT HEAD =	0.82833E-04		CONSTANT HEAD =	0.85150E-17	
0	TOTAL IN = 0.99274		0	TOTAL IN = 0.12021E-10	
0	OUT:		0	OUT:	
----		----			
STORAGE =	0.30647E-01		STORAGE =	0.48547E-13	
CONSTANT HEAD =	0.27702E-03		CONSTANT HEAD =	0.16152E-13	
0	TOTAL OUT = 0.30924E-01		0	TOTAL OUT = 0.64698E-13	
0	IN - OUT = 0.96182		0	IN - OUT = 0.11956E-10	
0	PERCENT DISCREPANCY =	187.92	0	PERCENT DISCREPANCY =	197.86

p=2/9, i=4, realization 5

VOLUMETRIC BUDGET FOR ENTIRE MODEL AT END OF TIME STEP 50 IN STRESS PERIOD 1

0	CUMULATIVE VOLUMES	L**3	RATES FOR THIS TIME STEP	L**3/T	
IN:		IN:			
---		---			
STORAGE =	1.0012		STORAGE =	0.16728E-19	
CONSTANT HEAD =	19.393		CONSTANT HEAD =	0.75430E-16	
0	TOTAL IN = 20.394		0	TOTAL IN = 0.75447E-16	
0	OUT:		0	OUT:	
----		----			
STORAGE =	0.12440E-02		STORAGE =	0.97264E-23	
CONSTANT HEAD =	22.778		CONSTANT HEAD =	0.46364E-16	
0	TOTAL OUT = 22.779		0	TOTAL OUT = 0.46364E-16	
0	IN - OUT = -2.3848		0	IN - OUT = 0.29083E-16	
0	PERCENT DISCREPANCY =	-11.05	0	PERCENT DISCREPANCY =	47.75

p=2/9, i=3, realization 1

VOLUMETRIC BUDGET FOR ENTIRE MODEL AT END OF TIME STEP 50 IN STRESS PERIOD 1

CUMULATIVE VOLUMES		L**3	RATES FOR THIS TIME STEP		L**3/T
IN:			IN:		
---			---		
STORAGE =	1.0021		STORAGE =	0.26149E-10	
CONSTANT HEAD =	0.91251E-03		CONSTANT HEAD =	0.10131E-13	
0	TOTAL IN = 1.0030		0	TOTAL IN = 0.26160E-10	
0	OUT:		0	OUT:	
----			----		
STORAGE =	0.30443E-01		STORAGE =	0.10685E-12	
CONSTANT HEAD =	0.32935		CONSTANT HEAD =	0.12522E-09	
0	TOTAL OUT = 0.35979		0	TOTAL OUT = 0.12533E-09	
0	IN - OUT = 0.64325		0	IN - OUT = -0.99170E-10	
0	PERCENT DISCREPANCY =	94.40	0	PERCENT DISCREPANCY =	-130.93

p=2/9, i=3, realization 2

VOLUMETRIC BUDGET FOR ENTIRE MODEL AT END OF TIME STEP 50 IN STRESS PERIOD 1

CUMULATIVE VOLUMES		L**3	RATES FOR THIS TIME STEP		L**3/T
IN:			IN:		
---			---		
STORAGE =	1.0077		STORAGE =	0.35562E-11	
CONSTANT HEAD =	0.52055E-02		CONSTANT HEAD =	0.37726E-12	
0	TOTAL IN = 1.0129		0	TOTAL IN = 0.39335E-11	
0	OUT:		0	OUT:	
----			----		
STORAGE =	0.13535E-01		STORAGE =	0.34740E-14	
CONSTANT HEAD =	0.41491E-01		CONSTANT HEAD =	0.48269E-11	
0	TOTAL OUT = 0.55026E-01		0	TOTAL OUT = 0.48303E-11	
0	IN - OUT = 0.95787		0	IN - OUT = -0.89684E-12	
0	PERCENT DISCREPANCY =	179.39	0	PERCENT DISCREPANCY =	-20.47

p=2/9, i=3, realization 3

VOLUMETRIC BUDGET FOR ENTIRE MODEL AT END OF TIME STEP 50 IN STRESS PERIOD 1

CUMULATIVE VOLUMES		L**3	RATES FOR THIS TIME STEP		L**3/T
IN:			IN:		
---			---		
STORAGE =	1.0592		STORAGE =	0.10465E-13	
CONSTANT HEAD =	0.42847E-02		CONSTANT HEAD =	0.67087E-16	
0	TOTAL IN = 1.0635		0	TOTAL IN = 0.10532E-13	
0	OUT:		0	OUT:	
----			----		
STORAGE =	0.64387E-01		STORAGE =	0.31895E-16	
CONSTANT HEAD =	0.38503E-01		CONSTANT HEAD =	0.13964E-13	
0	TOTAL OUT = 0.10289		0	TOTAL OUT = 0.13996E-13	
0	IN - OUT = 0.96059		0	IN - OUT = -0.34635E-14	
0	PERCENT DISCREPANCY =	164.71	0	PERCENT DISCREPANCY =	-28.24

p=1/9, i=2, realization 1

VOLUMETRIC BUDGET FOR ENTIRE MODEL AT END OF TIME STEP 50 IN STRESS PERIOD 1

0	CUMULATIVE VOLUMES	L**3	RATES FOR THIS TIME STEP	L**3/T
IN:		IN:		
---		---		
STORAGE =	1.0831	STORAGE =	0.61378E-11	
CONSTANT HEAD =	0.15195E-04	CONSTANT HEAD =	0.47128E-14	
0	TOTAL IN = 1.0831	0	TOTAL IN = 0.61425E-11	
0	OUT:	0	OUT:	
---		---		
STORAGE =	0.86145E-01	STORAGE =	0.33848E-13	
CONSTANT HEAD =	0.26929E-02	CONSTANT HEAD =	0.86502E-12	
0	TOTAL OUT = 0.88838E-01	0	TOTAL OUT = 0.89887E-12	
0	IN - OUT = 0.99431	0	IN - OUT = 0.52436E-11	
0	PERCENT DISCREPANCY =	169.68	PERCENT DISCREPANCY =	148.94

p=1/9, i=2, realization 3

VOLUMETRIC BUDGET FOR ENTIRE MODEL AT END OF TIME STEP 100 IN STRESS PERIOD 1

0	CUMULATIVE VOLUMES	L**3	RATES FOR THIS TIME STEP	L**3/T
IN:		IN:		
---		---		
STORAGE =	1.0873	STORAGE =	0.10498E-06	
CONSTANT HEAD =	0.12043E-03	CONSTANT HEAD =	0.70802E-11	
0	TOTAL IN = 1.0875	0	TOTAL IN = 0.10499E-06	
0	OUT:	0	OUT:	
---		---		
STORAGE =	0.10692	STORAGE =	0.16992E-08	
CONSTANT HEAD =	0.23405E-02	CONSTANT HEAD =	0.23393E-08	
0	TOTAL OUT = 0.10926	0	TOTAL OUT = 0.40384E-08	
0	IN - OUT = 0.97821	0	IN - OUT = 0.10095E-06	
0	PERCENT DISCREPANCY =	163.48	PERCENT DISCREPANCY =	185.18

p=1/9, i=2, realization 4

VOLUMETRIC BUDGET FOR ENTIRE MODEL AT END OF TIME STEP 50 IN STRESS PERIOD 1

0	CUMULATIVE VOLUMES	L**3	RATES FOR THIS TIME STEP	L**3/T
IN:		IN:		
---		---		
STORAGE =	1.0837	STORAGE =	0.18218E-12	
CONSTANT HEAD =	0.18916E-02	CONSTANT HEAD =	0.16473E-13	
0	TOTAL IN = 1.0856	0	TOTAL IN = 0.19865E-12	
0	OUT:	0	OUT:	
---		---		
STORAGE =	0.85402E-01	STORAGE =	0.12376E-13	
CONSTANT HEAD =	1.0765	CONSTANT HEAD =	0.81860E-10	
0	TOTAL OUT = 1.1619	0	TOTAL OUT = 0.81873E-10	
0	IN - OUT = -0.76323E-01	0	IN - OUT = -0.81674E-10	
0	PERCENT DISCREPANCY =	-6.79	PERCENT DISCREPANCY =	-199.0

Appendix E: Data

p	i	Rep	$\ln(K_{\text{eff},x})$	$\ln(K_{\text{eff},y})$	λ_{eff}	$\ln(K_{\text{slug}})$	r_{norm}	λ_r	S
8/9	5	1	-0.94	-0.95	1.01	-0.90	0.93	0.92	9.41E-04
8/9	5	2	-0.95	-0.94	0.99	-0.75	0.93	0.97	1.71E-03
8/9	5	3	-0.95	-0.94	0.99	-0.68	0.94	1.00	1.23E-03
7/9	5	1	-2.32	-2.42	1.11	-2.43	0.92	0.90	1.07E-06
7/9	5	2	-2.44	-2.24	0.82	-1.87	0.87	0.96	3.23E-04
7/9	5	3	-2.42	-2.43	1.01	-1.67	0.93	0.91	8.53E-03
6/9	5	1	-4.38	-4.50	1.12	-5.37	0.76	0.68	1.29E-17
6/9	5	2	-4.48	-4.69	1.23	-3.77	0.90	0.92	5.08E-03
6/9	5	3	-4.52	-4.35	0.84	-5.12	0.13	0.21	2.01E-18
5/9	5	1	-7.31	-7.45	1.15	-10.27	0.04	0.12	1.00E-20
5/9	5	2	-7.56	-8.03	1.60	-6.68	0.72	0.87	5.40E-03
5/9	5	3	-7.25	-7.67	1.52	-6.83	0.75	0.91	3.18E-05
4/9	5	1	-12.22	-11.49	0.48	-20.26	0.69	0.72	1.02E-10
4/9	5	2	-10.94	-10.89	0.95	-16.18	0.03	0.07	7.94E-15
4/9	5	3	-12.44	-12.27	0.84	-10.39	0.28	0.40	1.61E-01
3/9	5	1	-18.43	-19.99	4.79	-16.61	0.19	0.38	2.10E-04
3/9	5	2	-18.69	-18.66	0.96	-21.67	0.01	0.03	1.16E-10
3/9	5	3	-19.58	-17.03	0.08	-23.17	0.09	0.12	2.06E-10
2/9	5	1	-26.50	-31.56	158.16	-30.70	0.03	0.07	6.29E-11
2/9	5	2	-25.66	-32.05	590.91	-40.42	0.02	0.02	1.77E-10
2/9	5	3	-26.11	-28.56	11.65	-32.45	0.01	0.01	9.85E-11
1/9	5	1	ND	ND	ND	-39.50	0.00	ND	1.73E-13
1/9	5	2	ND	ND	ND	-42.57	0.04	ND	2.66E-11
1/9	5	3	ND	ND	ND	-34.64	0.01	ND	4.52E-15
8/9	4	1	-0.76	-0.72	0.97	-0.62	0.96	1.00	1.99E-04
8/9	4	2	-0.77	-0.72	0.95	-0.53	0.96	1.00	1.47E-03
8/9	4	3	-0.77	-0.72	0.95	-0.61	0.95	1.00	4.08E-05
7/9	4	1	-1.96	-1.89	0.93	-2.58	0.93	1.02	1.85E-03
7/9	4	2	-1.79	-1.89	1.11	-2.80	0.87	1.02	1.20E-10
7/9	4	3	-1.81	-1.89	1.08	-2.05	0.69	0.53	1.51E-09
6/9	4	1	-3.19	-3.29	1.10	-2.87	0.56	0.96	3.97E-05
6/9	4	2	-3.74	-3.27	0.62	-2.65	0.50	1.17	4.33E-04
6/9	4	3	-3.40	-3.41	1.01	-2.88	0.24	1.80	4.30E-03
5/9	4	1	-6.46	-5.80	0.52	-7.56	0.04	1.25	1.00E-20
5/9	4	2	-5.63	-5.73	1.10	-6.15	0.87	0.98	1.48E-01
5/9	4	3	-5.96	-6.47	1.67	-8.62	0.15	0.38	1.00E-20

p	i	Rep	ln(K_{eff,x})	ln(K_{eff,y})	λ_{eff}	ln(K_{slug})	r_{norm}	λ_r	S
4/9	4	1	-9.36	-9.28	0.92	-16.08	0.21	1.06	1.00E-20
4/9	4	2	-9.90	-8.77	0.32	-12.00	0.06	0.17	8.24E-19
4/9	4	3	-9.87	-10.36	1.63	-13.02	0.01	1.00	1.00E-20
3/9	4	1	-14.09	-14.25	1.18	-23.67	0.01	1.50	1.16E-10
3/9	4	2	-13.00	-12.97	0.97	-13.92	0.13	0.86	7.03E-10
3/9	4	3	-16.85	-13.14	0.02	-10.98	0.05	0.85	3.70E-12
2/9	4	1	-18.70	-25.92	1372.53	-20.54	0.07	6.00	2.18E-10
2/9	4	2	-21.73	-21.52	0.81	-16.17	0.03	0.63	1.34E-20
2/9	4	3	-26.80	-20.82	0.00	-34.34	0.01	1.00	1.00E-20
1/9	4	1	ND	ND	ND	-51.78	0.04	ND	1.00E-20
1/9	4	2	ND	ND	ND	-30.45	0.03	ND	3.45E-04
1/9	4	3	ND	ND	ND	-28.17	0.01	ND	1.55E-10
8/9	3	1	-0.56	-0.60	1.04	-1.45	0.94	0.99	5.12E-03
8/9	3	2	-0.59	-0.57	0.98	-0.55	0.93	1.02	3.53E-04
8/9	3	3	-0.57	-0.55	0.98	-0.29	0.94	1.01	9.98E-04
7/9	3	1	-1.33	-1.41	1.08	-1.16	0.94	1.04	5.72E-04
7/9	3	2	-1.36	-1.34	0.98	-0.80	0.95	1.00	1.29E-03
7/9	3	3	-1.30	-1.35	1.06	-2.16	0.95	0.97	1.36E-03
6/9	3	1	-2.67	-2.47	0.82	-2.54	0.83	1.12	3.39E-04
6/9	3	2	-2.83	-2.24	0.55	-3.64	0.76	0.99	4.19E-07
6/9	3	3	-2.43	-2.55	1.12	-4.10	0.85	0.96	1.41E-05
5/9	3	1	-3.95	-4.50	1.72	-5.53	0.76	0.70	3.35E-02
5/9	3	2	-4.36	-4.17	0.83	-7.73	0.36	0.69	9.14E-03
5/9	3	3	-5.03	-3.47	0.21	-5.28	0.75	1.50	3.32E-07
4/9	3	1	-6.94	-5.57	0.25	-10.59	0.13	1.35	5.73E-04
4/9	3	2	-6.36	-5.82	0.58	-3.94	0.29	0.03	1.16E-01
4/9	3	3	-7.11	-6.76	0.70	-4.72	0.72	1.01	7.66E-01
3/9	3	1	-11.18	-10.34	0.43	-14.02	0.27	1.15	1.49E-02
3/9	3	2	-11.10	-9.17	0.15	-7.82	0.61	0.74	8.01E-04
3/9	3	3	-9.78	-11.19	4.10	-11.20	0.29	1.52	4.64E-01
2/9	3	1	-14.79	-14.79	0.99	-19.42	0.05	1.75	6.88E-11
2/9	3	2	-16.15	-16.21	1.07	-19.85	0.09	1.59	6.62E-18
2/9	3	3	-17.27	-15.12	0.12	-26.40	0.08	1.11	7.15E-07

p	l	Rep	$\ln(K_{\text{eff},x})$	$\ln(K_{\text{eff},y})$	λ_{eff}	$\ln(K_{\text{slug}})$	r_{norm}	λ_r	S
1/9	3	1	ND	ND	ND	-32.83	0.20	ND	2.95E-02
1/9	3	2	ND	ND	ND	-38.18	0.11	ND	9.13E-11
1/9	3	3	ND	ND	ND	-34.42	0.11	ND	1.10E-08
8/9	2	1	-0.42	-0.46	1.04	-0.13	0.95	1.00	3.63E-04
8/9	2	2	-0.42	-0.46	1.04	-0.25	0.95	1.00	6.41E-04
8/9	2	3	-0.39	-0.47	1.08	-0.11	0.96	1.00	5.51E-04
7/9	2	1	-0.87	-0.95	1.07	-0.33	0.96	0.99	7.05E-04
7/9	2	2	-0.96	-0.88	0.92	-3.25	0.74	0.94	9.06E-08
7/9	2	3	-0.98	-0.87	0.89	-0.93	0.64	0.97	3.55E-05
6/9	2	1	-1.77	-1.58	0.82	-0.58	0.94	1.00	1.50E-03
6/9	2	2	-1.63	-1.67	1.04	-0.65	0.80	1.10	3.31E-03
6/9	2	3	-1.82	-1.47	0.70	-0.82	0.91	1.05	3.00E-03
5/9	2	1	-2.20	-3.11	2.49	-0.95	0.78	0.70	9.90E-03
5/9	2	2	-2.64	-2.73	1.09	-8.76	0.11	0.93	2.28E-10
5/9	2	3	-2.47	-3.30	2.28	-2.10	0.87	0.86	7.73E-03
4/9	2	1	-4.41	-3.60	0.45	-2.39	0.78	0.70	4.35E-03
4/9	2	2	-4.30	-5.65	3.89	-9.59	0.21	0.04	2.27E-02
4/9	2	3	-3.70	-3.91	1.24	-2.01	0.76	1.10	2.22E-02
3/9	2	1	-6.37	-6.94	1.77	-10.01	0.14	1.54	1.30E-10
3/9	2	2	-6.75	-6.59	0.86	-8.67	0.16	2.00	6.89E-10
3/9	2	3	-6.64	-6.14	0.60	-7.27	0.17	1.66	3.50E-08
2/9	2	1	-9.54	-11.74	9.03	-4.34	0.52	0.53	1.67E-01
2/9	2	2	-11.55	-13.32	5.88	-9.03	0.54	0.92	1.24E-01
2/9	2	3	-8.04	-9.82	5.93	-5.58	0.45	0.39	1.68E-02
1/9	2	1	-15.28	-15.40	1.12	-19.00	0.08	1.85	1.68E-09
1/9	2	2	-17.52	-17.60	1.09	-19.73	0.20	0.42	1.34E-09
1/9	2	3	-13.95	-17.74	44.51	-10.67	0.13	0.38	5.95E-09
8/9	1	1	-0.41	-0.29	0.89	-0.10	0.81	0.67	5.32E-04
8/9	1	2	-0.36	-0.35	0.99	-0.09	0.80	1.49	5.02E-04
8/9	1	3	-0.28	-0.41	1.14	-0.09	0.80	1.49	5.18E-04
7/9	1	1	-0.47	-0.57	1.10	-0.07	0.97	1.00	4.64E-04
7/9	1	2	-0.53	-0.48	0.95	-0.08	0.96	1.00	4.68E-04
7/9	1	3	-0.45	-0.57	1.12	-0.10	0.80	1.48	5.58E-04
6/9	1	1	-0.64	-0.87	1.25	-0.08	0.97	0.99	4.61E-04
6/9	1	2	-0.93	-0.48	0.64	-0.21	0.88	1.01	6.06E-04
6/9	1	3	-0.76	-0.97	1.23	-2.30	0.94	1.00	6.11E-05
5/9	1	1	-2.30	-0.85	0.23	-0.17	0.72	2.03	8.71E-04
5/9	1	2	-1.24	-1.06	0.84	-2.34	0.75	1.47	2.21E-04
5/9	1	3	-0.92	-1.66	2.10	-2.20	0.91	0.99	7.48E-05

p	l	Rep	ln(K _{eff,x})	ln(K _{eff,y})	λ _{eff}	ln(K _{slug})	r _{norm}	λ _r	S
4/9	1	1	-2.72	-0.48	0.11	-0.38	0.43	1.65	1.70E-03
4/9	1	2	-1.80	-2.04	1.28	-1.05	0.20	0.04	1.00E-03
4/9	1	3	-2.10	-2.83	2.08	-3.94	0.44	1.68	8.09E-04
3/9	1	1	-2.82	-2.14	0.51	-5.79	0.47	0.51	1.78E-04
3/9	1	2	-1.76	-4.14	10.84	-0.30	0.80	0.69	1.83E-03
3/9	1	3	-2.59	-2.50	0.91	-1.76	0.69	2.24	6.12E-04
2/9	1	1	-4.52	-6.30	5.96	-1.15	0.79	0.79	3.50E-03
2/9	1	2	-3.89	-5.56	5.30	-4.45	0.71	1.80	2.21E-04
2/9	1	3	-3.84	-3.90	1.06	-2.92	0.58	0.89	2.70E-04
1/9	1	1	-6.23	-10.14	49.99	-0.76	0.41	0.66	1.28E-02
1/9	1	2	-7.56	-4.26	0.04	-0.76	0.37	1.28	1.29E-02
1/9	1	3	-9.02	-5.29	0.02	-13.10	0.38	1.37	6.62E-05

*Hydraulic conductivity units meter/second, S=storativity

Results for 100 simulations in a p=4/9, i=5, b=3 multifractal field:

ln(K _{eff})				ln(K _{slug})			
-12.05	-12.75	-12.92	-12.37	-10.45	-11.73	-21.95	-8.78
-11.39	-11.25	-10.98	-11.97	-10.76	-13.55	-12.69	-24.90
-11.97	-11.71	-11.78	-11.80	-15.95	-21.05	-18.56	-13.28
-11.08	-10.55	-12.22	-11.09	-10.91	-20.51	-7.92	-17.13
-12.16	-10.75	-10.94	-11.55	-9.97	-10.10	-11.40	-11.57
-12.05	-13.18	-12.44	-11.98	-10.97	-17.96	-8.82	-11.40
-11.69	-11.98	-12.95	-12.54	-12.44	-8.45	-9.83	-9.91
-11.86	-11.79	-12.31	-12.72	-13.27	-13.91	-20.26	-12.33
-12.01	-11.43	-11.74	-13.78	-22.40	-16.57	-16.18	-10.75
-12.23	-11.15	-11.94	-11.25	-11.86	-14.86	-10.39	-9.89
-11.11	-12.18	-13.04	-11.42	-13.51	-10.41	-18.27	-16.34
-11.23	-12.11	-11.22	-11.26	-10.58	-10.42	-10.08	-18.48
-12.26	-12.77	-11.68	-11.69	-9.30	-16.41	-10.77	-13.71
-11.41	-11.09	-11.58	-12.49	-8.12	-21.08	-12.33	-21.76
-11.79	-11.59	-11.30	-11.32	-24.20	-11.80	-17.42	-20.36
-11.08	-11.24	-12.26	-12.91	-13.16	-16.82	-12.36	-14.68
-11.11	-11.38	-12.42	-11.74	-16.54	-9.13	-13.54	-14.24
-11.97	-12.97	-11.98	-12.17	-11.60	-16.96	-11.73	-11.69
-10.57	-12.44	-11.66	-11.83	-11.07	-18.94	-9.23	-9.86
-12.15	-11.33	-12.20	-11.72	-9.08	-14.52	-10.64	-23.03
-11.61	-11.51	-10.89	-11.43	-12.29	-17.00	-9.37	-9.23
-11.23	-10.39	-12.27	-10.84	-14.05	-18.61	-13.72	-10.79
-13.12	-12.14	-11.66	-11.64	-17.00	-18.02	-11.89	-10.97
-12.34	-11.89	-12.04	-11.64	-17.58	-11.62	-9.83	-11.46
-11.54	-11.49	-11.35	-12.83	-17.16	-10.29	-13.53	-16.34

Vita

Richard Donat was born in Fayetteville, Arkansas on June 30th 1980. His love of geology and nature was developed as a child by his father who would take him to Crater of Diamonds in Arkansas to search for diamonds. Upon entering the University of Arkansas in the Fall of 2002 he remained undecided on a major until he took a Geology 101 course with Professor Walter Manger. After this course he declared a major in geology gaining a specialty in hydrogeology as he progressed through the undergraduate curriculum. With various projects on the springs around NW Arkansas he began to develop a love for problem solving, nature, and clean water as a viable resource. He decided after finishing his undergraduate degree at the University of Arkansas that he would continue his education and get his masters with Dr. Edmund Perfect at the University of Tennessee. By working with Dr. Perfect and other faculty at the University of Tennessee he has developed lifelong skills of problem solving, critical thinking, and furthered his understanding on the subject of groundwater which he greatly appreciates. Future plans include moving to San Antonio, Texas to work on the Edwards Aquifer, as well as, working on furthering and providing clean sustainable drinking water to communities around the United States and possibly the world.